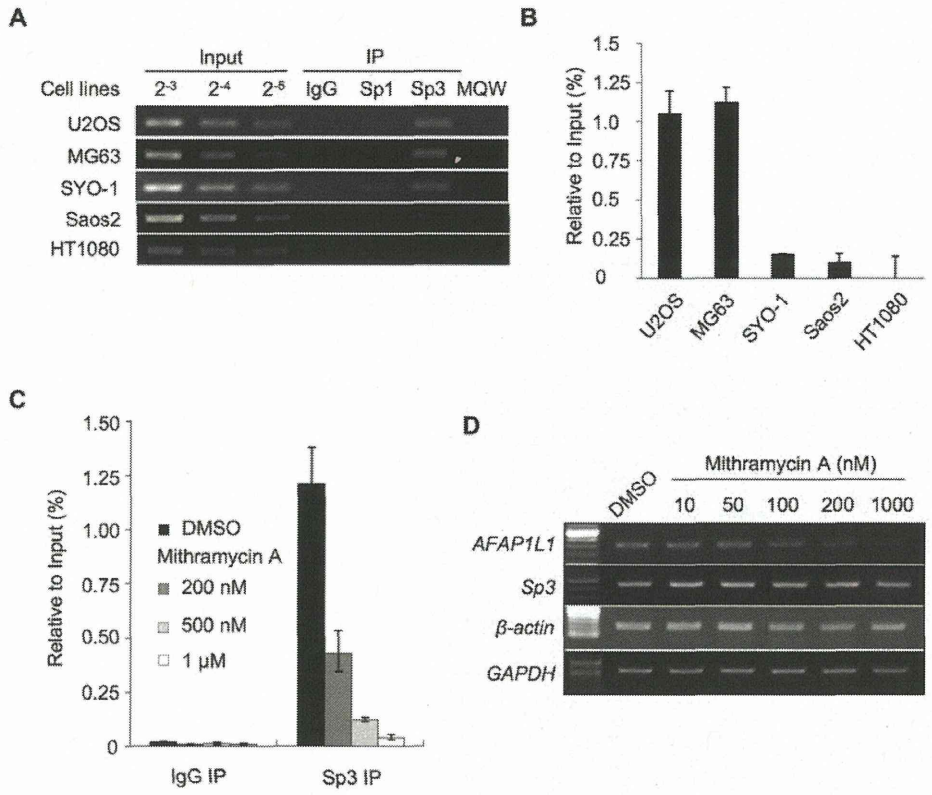

Figure 5. Identification of Sp3 as a major transcription factor for *AFAP1L1*. (A) and (B) Binding of Sp transcription factors to the core-promoter region of the *AFAP1L1* gene *in vitro*. ChIP assays were performed using anti-Sp1 and anti-Sp3 antibodies or control IgG and the precipitated DNA was PCR-amplified using a pair of primers located in the core-promoter region (Table S1) (A), and the precipitated genome was quantified by qPCR (B). (C) The effect of mithramycin A treatment on Sp3 binding. U2OS cells were treated with mithramycin A or DMSO for 48 h, and immunoprecipitated DNA by Sp3 antibody was quantified by qPCR. (D) The effect of mithramycin A on the expression of the *AFAP1L1* gene. RNA was extracted from U2OS cells treated with mithramycin A or DMSO for 48 h, and RT-PCR was performed to semi-quantify the expression of each gene. The *β-actin* and *GAPDH* genes were used as a control. Error bars indicate standard deviations.
doi:10.1371/journal.pone.0049709.g005

pLenti6/V5-DEST (Invitrogen). pLenti6/V5-GW/*lacZ* (Invitrogen) and pLenti6/V5-DEST/EGFP were used as lentiviral controls. Using the ViraPower Lentiviral Expression System (Invitrogen), U2OS cells were infected with viral supernatant containing the siRNA-resistant *Sp3(li-1)* or control gene according to the manufacturer's instructions.

Matrigel invasion assay

At 48 h after siRNA treatment, cells were collected and cultured in BioCoat Matrigel Invasion Chambers (BD Biosciences) and 8-μm pore Control Cell Culture Inserts (BD Biosciences) as described previously [1]. Cells (5×10^4) were seeded in each chamber in triplicate and incubated for 22 h. Then cells were fixed and migrating cells were counted in five random fields under the microscope at ×100 magnification.

Results

AFAP1L1 mRNA expression in sarcoma cell lines

First, we checked *AFAP1L1* expression in sarcoma cell lines by RT-PCR and qPCR. *AFAP1L1* was expressed strongly in U2OS and MG63 cells, very weakly in SYO-1 and Saos2 cells, and not at all in HT1080 cells (Fig. 1A–B). In the Western blot analysis, AFAP1L1 was detected in U2OS and MG63 cells but undetectable in SYO-1, Saos2 and HT1080 cells (Fig. 1C), indicating that the expression of AFAP1L1 was regulated differently among sarcomas at the transcriptional level.

AFAP1L1 promoter activity depends on the proximal conserved region

To identify the transcriptional regulatory elements of the *AFAPL1* gene, DNA fragments with various segments of the *AFAP1L1* promoter were cloned into the PGV-basic vector as described in the section of Materials and Methods. They were transfected into U2OS cells expressing endogenous AFAP1L1 and their luciferase activities were measured (Fig. 2A). The longest fragment showed the strongest promoter activity and shorter ones less, but the decrease was not remarkable until the fragment lost the region between −224 and −71 relative to TSS (Fig. 2A). By searching the CONSITE database [7], we found that the sequence from −150 to −40 was highly conserved in three species (Fig. 2B). Of note, within that conserved region two Ets-binding motifs (5′-(A/C)GGA(A/T)-3′) and two Sp1-binding motifs (5′-GGGCGG-3′) were identified. The proximal (−60 to −56) and distal (−102 to −97) Ets-binding motifs were designated Ets-binding site 1 (EBS1) and 2 (EBS2), respectively. The proximal Sp1-binding site (−86 to −76) contained two overlapping consensus sequences (−86 to −81 and −81 to −76) and was conserved completely in

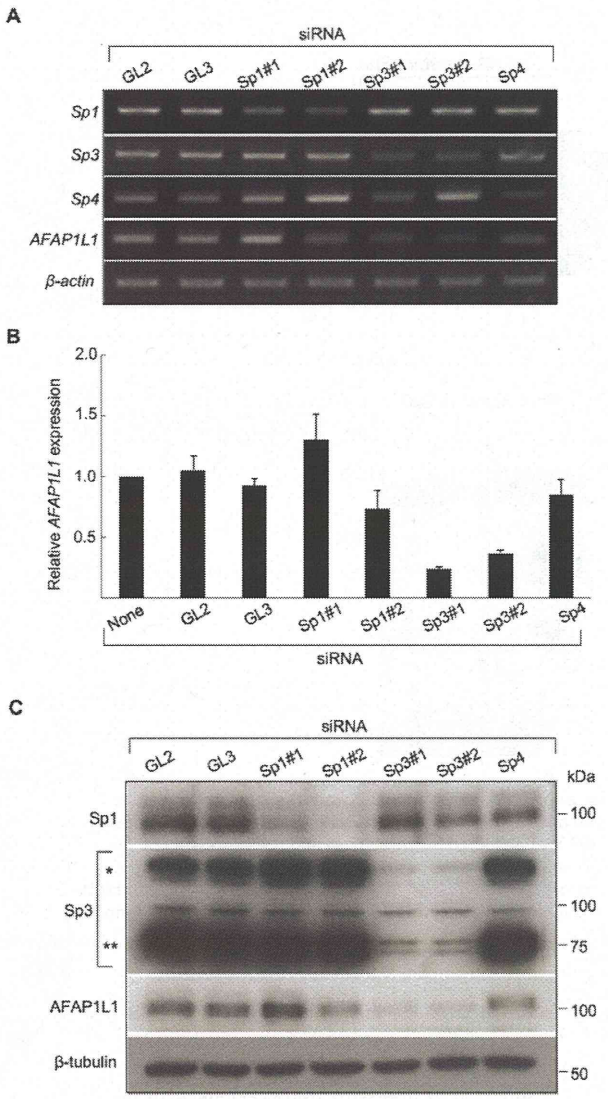

Figure 6. Linking of Sp3 with AFAP1L1 by siRNA experiments. (A) The specificity of siRNA. U2OS cells were treated with siRNA targeting *Sp1*, *Sp3*, or *Sp4* for 48 h, and the expression of these genes as well as the *AFAP1L1* gene was analyzed by PCR. Two different siRNAs targeting the *Sp1* and *Sp3* genes were designed and used. *β-actin* was used as a control. (B) Down-regulation of *AFAP1L1* expression by siRNA targeting the *Sp3* gene at the mRNA level. U2OS cells were treated with siRNAs targeting each gene for 48 h and the expression of *AFAP1L1* was analyzed by qPCR and indicated as fold changes relative to that in untreated cells. (C) Down-regulation of AFAP1L1 expression by siRNA targeting the *Sp3* gene at the protein level. U2OS cells were treated with siRNA targeting each gene for 72 h and proteins were extracted and used for Western blotting. β-tubulin was used as a control.
doi:10.1371/journal.pone.0049709.g006

all three species, and was designated SBS1. The distal Sp1-binding site (SBS2) spanning −102 to −97 was found only in the human genome. Several studies have shown that Ets and Sp proteins function together in the transcription of target genes [8,9], and therefore we focused on Ets and Sp transcription factors.

The Proximal Sp1-binding site is essential to *AFAP1L1* transcription

To investigate the role of Ets and Sp transcription factors in the promoter activity, four types of luciferase reporters with mutations in the conserved sequence of each binding site were constructed using PGV-(−224) as a template and designated PGV-mtEBS1, PGV-mtEBS2, PGV-mtSBS1, and PGV-mtSBS2. When EBS1 was mutated, the promoter activity was reduced by 50% compared to PGV-(−224), although PGV-(−71) which retained EBS1 also showed reduced activity (Fig. 3A). However, the effect was most remarkable when SBS1 was mutated, which resulted in a 75% reduction in promoter activity (Fig. 3A). This level was almost equivalent to that of PGV-(−53), which retained no EBSs or SBSs. Mutations in EBS2 or SBS2 had less significant effects on the promoter activity (Fig. 3A). These results suggested that although both Sp and Ets proteins might play roles in transcriptional regulation of the *AFAP1L1* gene, the Sp protein binding to SBS1 is the main factor driving the expression of *AFAP1L1*. Therefore, we focused on Sp proteins.

Sp1 and Sp3 transactivate the proximal *AFAP1L1* promoter

To determine whether Sp1 and/or Sp3 transactivate the promoter activity of the *AFAP1L1* gene, a luciferase assay was carried out using the Sp1 (pEVR2/Sp1) and Sp3 (pcDNA/Sp3(li-1)) expression vectors, which produce each protein effectively in transfected cells (Fig. S1). Co-transfection of the Sp1 or Sp3(li-1) expression vector increased the promoter activity of PGV-(−224) in a dose-dependent manner (Fig. 3B), suggesting Sp1 and Sp3 to function in the transactivation of *AFAP1L1*. Interestingly, co-transfection of the vector expressing a short form of Sp3, Sp3(si-1), significantly reduced the promoter activity of PGV-(−224) (Fig. S2). No significant effects were observed on the co-transfection of the Sp3(li-2) or Sp3(si-2) expression vector (data not shown).

Sp1 and Sp3 bind to *AFAP1L1*'s proximal promoter region

To elucidate whether Sp1 and Sp3 bind to SBS1 *in vitro*, EMSA was conducted using labeled SBS1 OND and U2OS nuclear extract. Using wild-type ONDs (SBS1WT), several shifted bands were observed (Fig. 4, *lane b*), among which three showed a decrease in intensity in competition with unlabeled SBS1WT in a dose-dependent manner (Fig. 4, *lanes c–d*). These three bands were not detected when labeled SBS1MUT was used instead of SBSWT for the assay (Fig. S3, *lanes f–h*). When unlabeled SBS1MUT was used as a competitor, no reduction in intensity was observed (Fig. 4, *lanes e* and *f*), suggesting that the bands were specific to SBS1 complexes. When the anti-Sp1 antibody was added to the OND/protein mixture, the intensity of the uppermost band decreased and a supershifted band was identified, whereas no remarkable changes were observed in the other two bands (Fig. 4, *lane g*; Fig. S3, *lane c*). The intensity of the uppermost band showed no change when an anti-Sp3 antibody was used but the other two bands showed a clear difference (Fig. 4, *lane h*; Fig. S3, *lane d*). The intensity of the middle band decreased and the lower band almost disappeared, which was associated with the appearance of two supershifted bands (Fig. 4, *lane h*). These changes were not observed when labeled SBS1MUT was used in the assay (Fig. S3, *lanes g–h*). No remarkable change was observed with the addition of control IgG (Fig. 4, *lane i*). These results suggested that the uppermost and lower two bands corresponded to Sp1- and Sp3-OND complexes, respectively, and therefore both Sp1 and Sp3 are able to bind to the proximal Sp1-binding site *in vitro*. Similar results were obtained when nuclear extracts were prepared from

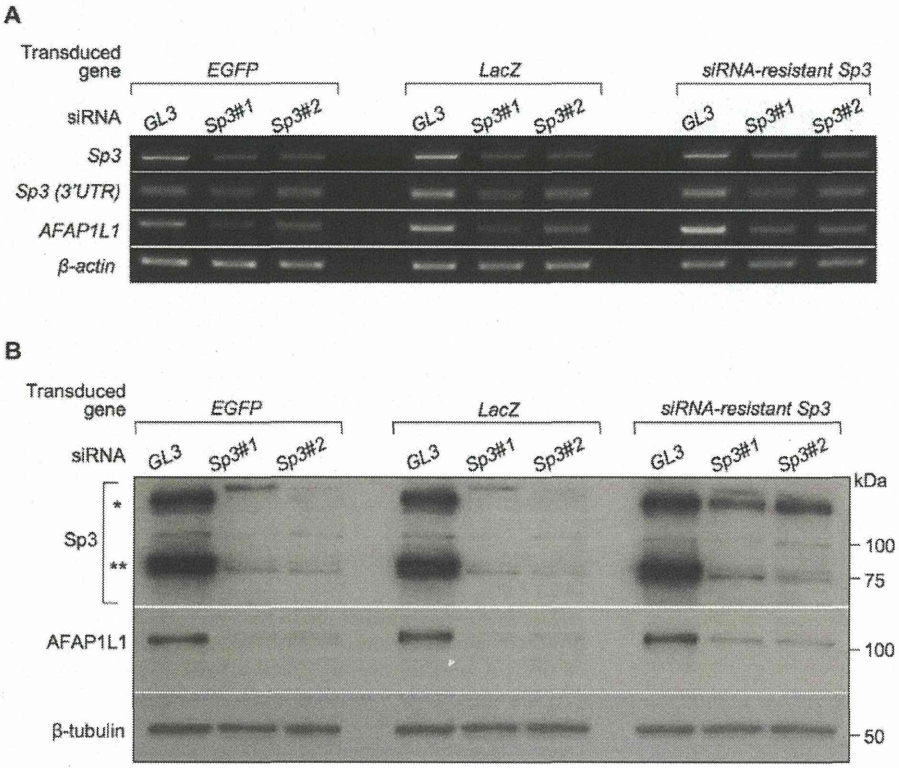

Figure 7. Restoration of down-regulated AFAP1L1 expression by an siRNA-resistant Sp3 expression vector. U2OS cells stably expressing the Sp3 mRNA resistant to Sp3#1 and Sp3#2 siRNA was established and treated with these siRNAs. U2OS cells stably expressing the *EGFP* or *LacZ* gene were employed as a control. After 48-h-treatment with siRNAs, RNA was extracted from each cell and the expression of *Sp3* and *AFAP1L1* was analyzed by RT-PCR (A). Knocking down of the endogenous *Sp3* gene was confirmed by PCR using a set of primers located in the 3′ UTR of the *Sp3* gene (Table S1). The *β-actin* gene was used as a control. Protein was extracted after 72 h of treatment and used for Western blotting (B). β-tubulin was used as a control. Error bars indicate standard deviations. Single and double asterisks indicate the long and short forms of the Sp3 protein, respectively.
doi:10.1371/journal.pone.0049709.g007

MG63 cells, which were strongly positive for AFAP1L1 (Fig. S4, *lanes h–n*). Interestingly, similar results were also obtained when nuclear extracts were prepared from SYO-1 cells, which were very weakly positive for AFAP1L1 (Fig. S4, *lanes a–g*). These results suggested that the expression of AFAP1L1 *in vivo* was regulated by not only the *cis*-element but also other factors such as chromatic modification.

Sp3 regulates the transcription of the *AFAP1L1* gene by binding to the endogenous promoter region

To investigate whether Sp1 and/or Sp3 bind to SBS1 *in vivo*, ChIP assays were conducted using four cell lines in which the gene expression of AFAP1L1 differed considerably; U2OS (strong), MG63 (strong), SYO-1 (very weak), Saos2 (very weak) and HT1080 (null) (Fig. 1A). We found that Sp3 bound to the *AFAP1L1* promoter region strongly in U2OS and MG63 cells (Fig. 5A), but weakly in SYO-1 and Saos2 cells. No binding of Sp3 to the proximal promoter region was detected in HT1080 cells. Binding of Sp1 was below the significant level by as determined by qPCR (data not shown). Quantitative analyses showed a clear correlation between the binding of Sp3 and the expression level of *AFAP1L1* (Fig. 1A and Fig. 5B). To exclude the possibility that this difference in the binding of Sp3 to the promoter is due to mutations in binding sites, we checked the genomic DNA of U2OS, MG63, SYO-1 and HT1080. No mutations were found in the proximal promoter including EBS1, EBS2, SBS1 and SBS2 in any of the cell lines investigated (data not shown).

Mithramycin A is an aureolic acid antibiotic, which inhibits gene expression by displacing transcriptional activators like the Sp protein family that bind to GC-rich regions of promoters [10,11]. Treatment with mithramycin A inhibited the binding of Sp3 to the promoter region of the *AFAP1L1* gene in a dose-dependent manner (Fig. 5C). Consistent with this finding, the treatment with Mithramycin A reduced the mRNA expression of *AFAP1L1* without changing that of Sp3 in U2OS cells (Fig. 5D). Similar results were observed in another AFAP1L1-positive cell line, MG63 cells (Fig. S5). These results indicate that the binding of Sp3 to SBS1 is a prerequisite for *AFAP1L1* transcription, the level of which is regulated by the extent of the binding. Total and nuclear protein levels of Sp3 are almost the same in these four cell lines (Fig. S6A–B), suggesting the existence of undiscovered mechanisms that regulate the binding of Sp3 to SBS1. The luciferase assays suggested the involvement of the Ets protein family in the regulation of *AFAP1L1* transcription (Fig. 3A). Transfection of a dominant-negative Ets vector significantly reduced *AFAP1L1* promoter activity, also suggesting the Ets family to participate in the transcription of *AFAP1L1* (Fig. S7A). Interestingly, transfection of ELK1, another member of the Ets family, reduced *AFAP1L1* promoter activity (Fig. S7A), and we found that forced expression of ELK1 up-regulated the two short isoforms of Sp3 (Fig. S7B),

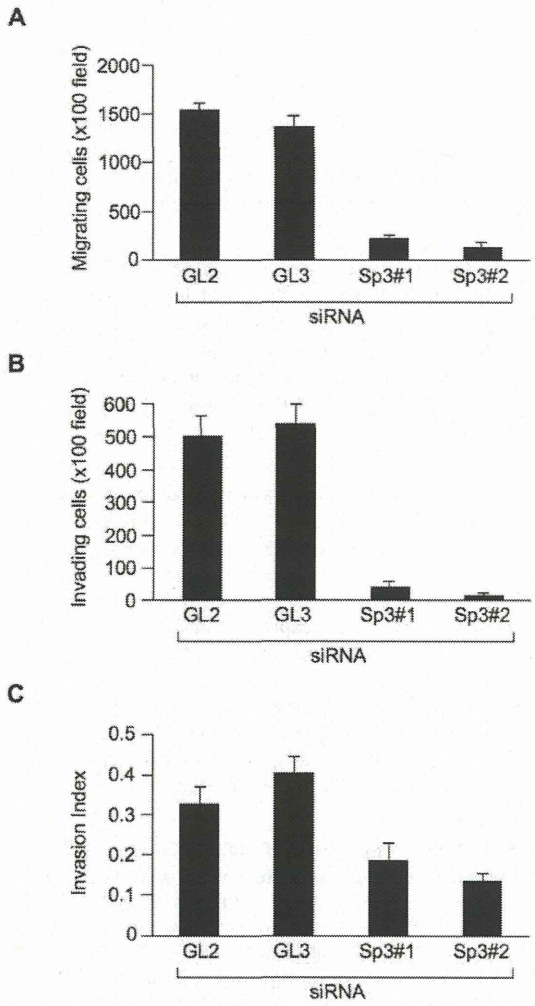

Figure 8. Inhibition of Sp3 expression reduces cell migration and invasiveness in U2OS cells. Numbers of cells migrating through the uncoated 8-micron membrane pores (A) and through the Matrigel-coated membranes (B) were counted in five randomly chosen fields at a magnification of ×100. (C) A cell invasion index was calculated as the ratio of the number of cells migrating through the matrigel to the number migrating through the uncoated membrane.
doi:10.1371/journal.pone.0049709.g008

which may be responsible for the reduction in promotor activity, based on the results of co-transfection experiments (Fig. S2). mRNA expression levels of *ELK1* and *ELK4* showed no significant differences among sarcoma cell lines irrespective of the AFAP1L1 expression level (Fig. S7C).

Sp3 is essential to the expression of AFAP1L1

Finally, siRNA was employed to investigate the role of Sp3 in AFAP1L1 transcription *in vivo*. In U2OS cells, siRNA targeting each of Sp1, Sp3, and Sp4 significantly reduced the expression of the targeted gene, but only the siRNA targeting Sp3 consistently reduced the expression of the *AFAP1L1* gene (Fig. 6A), which was confirmed by quantitative analyses (Fig. 6B). Specific reduction of *AFAP1L1* expression by siRNA against Sp3 was further confirmed at the protein level (Fig. 6C). These effects of siRNA against Sp3 were also confirmed in other cell lines (MG63 and SYO-1) at the mRNA level (Fig. S8A–D). This phenomenon was also observed in prostate cancer PC-3 cells (Fig. S9), indicating that the transcriptional role of Sp3 for the *AFAP1L1* gene is not restricted to sarcoma cells. To exclude the off-target effect of siRNA, a rescue experiment was carried out. Pre-induction of siRNA-resistant Sp3 using a lentivirus partially rescued *AFAP1L1* expression after Sp3 siRNA treatment (Fig. 7A–B), indicating that the reduction in AFAP1L1 expression cause by siRNA for Sp3 is due to a direct effect on the Sp3 gene.

Functional relevance of Sp3 to AFAP1L1

We have shown that the induction of AFAP1L1 expression increased cell motility and invasiveness in sarcoma cells [1]. Inhibition of Sp3 expression with siRNA also reduced the motility and invasiveness of U2OS cells, suggesting a functional link between Sp3 and AFAP1L1 (Fig. 8).

Discussion

In the present study, we have found that Sp3 plays a critical role in the transcription of *AFAP1L1*, a gene associated with the metastasis of soft tissue spindle cell sarcomas [1]. Based on structural similarity, AFAP1, AFAP1L1 and AFAP1L2 belong to a family of new adaptor proteins. They all contain two pleckstrin homology domains flanking a serine/threonine-rich region, two Src homology (SH) 2-binding motifs and one or two SH3-binding motifs [1] [12] [13]. AFAP1, also known as AFAP-110, the most intensively investigated member of the family, is reported to have an intrinsic ability to alter actin filament integrity and may function as an adaptor protein by linking the Src family and/or other signaling proteins to actin filaments [13]. AFAP1L2, also termed XB130, has been cloned as an adaptor protein and Src kinase substrate and phosphorylated by RET/PTC, a genetically rearranged, constitutively active, thyroid- specific tyrosine kinase [14]. In contrast to AFAP1 and AFAP1L2, little is known about AFAP1L1. A recent study revealed that AFAP1L1 interacted with the SH3 domain of cortactin, an F-actin-binding protein [15] Although we had previously reported that AFAP1L1 was associated with the progression of sarcomas, how it functions in the invasiveness of tumor cells remains ill defined.

Sp3 is a member of the Sp/Kruppel-like factor (KLF) family. The Sp/KLF family recognizes GC/GT boxes and interacts with DNA through three zinc finger motifs [16]. Eight members of the Sp family, Sp1-8, have been reported. Sp1 was the first transcription factor identified and cloned among Sp family members [17] and has been intensively investigated. Since the DNA-binding domains of Sp1 and Sp3 share 90% homology in DNA sequence, they bind to the same DNA-binding site with similar affinity [16]. In spite of extensive studies on the Sp proteins, the difference in binding properties between Sp1 and Sp3 remains largely unknown. Notably, one study shows that promoters containing multiple adjacent Sp-binding sites form significantly more stable Sp3-DNA complexes than those with single Sp-binding sites, and as a consequence, Sp3 efficiently displaces Sp1 from preformed Sp1-DNA complexes from such sites [18]. Therefore, in *AFAP1L1*'s promoter region, the Sp3-SBS1 complexes might be more more stable than the Sp1-SBS1 complexes, because SBS1 contains two overlapping consensus Sp-binding sequences. The Sp3 protein has four isoforms; two long isoforms and two short isoforms [5]. All of them are derived from alternative translational start sites. The two long isoforms can act as transcriptional activators in certain settings, but the significance of the two small isoforms as transcriptional activators or inhibitors remains to be elucidated [5]. While investigating the

role of Sp3 and Ets in the *AFAP1L1* promoter's activity, we found that forced expression of ELK1, an Ets transcription factor, induced up-regulation of the two short isoforms of Sp3 and resulted in decreased *AFAP1L1* promoter activity (Fig. S7B). As forced expression of a short isoform (si-1) reduced the *AFAP1L1* promoter activity induced by endogenous factors (Fig. S2), si-1 may have a negative effect on the transcription of *AFAP1L1*.

Sp1 and Sp3 have been shown to be expressed ubiquitously and reported to regulate basal and constitutive expression of genes both in normal and cancerous tissues [19]. Several reports have referred to a correlation between Sp1 and Sp3 and tumor development, growth and metastasis. Sp1 is reported to be overexpressed and regulate vascular endothelial growth factor (VEGF) in gastric and shown to be linked to a poor prognosis [20]. Up-regulation of Sp1 expression has been also observed in thyroid [21] and colorectal cancer [22]. Sp3 enhances the growth of pancreatic cancer cells by suppressing p27 expression through interaction with GC-rich promoter elements [23]. In breast cancer, Sp3 accelerates tumor cell growth by acting as a repressor of TGF signaling [24]. A recent report demonstrated the expression of Sp3 to be an independent prognostic factor for the poor survival of head and neck cancer patients [25]. Of note, in the web database ONCOMINE (http://www.oncomine.org), upregulation of Sp3 expression in soft tissue sarcomas compared to normal connective tissue has been confirmed [26] [27].

Because the cause of sarcoma patients' death is uncurable distant metastasis in most cases, methods of both predicting and treating metastasis are urgently needed. Our findings may provide new insight regarding this clinical difficulty. Considering that Sp3 is expressed at higher levels in soft tissue sarcomas and transactivates the *AFAP1L1* gene, targeting Sp3 could be a powerful approach to treating advanced soft tissue sarcomas.

Supporting Information

Figure S1 Expression of exogenous Sp1 or Sp3 protein in 293T cells. 293T cells were transfected with each plasmid, as described in Materials and Methods, and the expression of the Sp1 or Sp3 protein was analyzed 24 h later. pRC/Sp3 lacks N-terminal part of the *Sp3* gene as described in *Experimental Procedures*. β-tubulin was used as an internal control. Single and double asterisks indicate the long and short forms of the Sp3 protein, respectively.
(TIF)

Figure S2 Isoform-dependent activity of Sp3 on *AFAP1L1* promoter. The luciferase reporter assay was performed as described in Fig. 3B. Reporter plasmids were co-transfected with either an empty, Sp1 or Sp3 expression vector. Error bars indicate the standard deviations.
(TIF)

Figure S3 Binding of Sp transcription factors to the wild-type, but not mutated Sp-binding site *in vitro*. Nuclear extracts were prepared from U2OS cells and used for EMSA with radiolabeled SBS1WT (*lane a–d*) or SBS1MUT (*lanes e–h*). A supershifted assay was performed with anti-Sp1 (*lane c* and *g*) or anti-Sp3 (*lane d* and *h*) antibody. Open and closed arrowheads indicate an Sp3-OND and Sp1-OND complex.
(TIF)

Figure S4 EMSA using nuclear extracts from cells expressing the *AFAP1L1* gene very weakly (SYO-1) and strongly (MG63). Nuclear extracts were prepared from SYO-1 and MG63 cells, and EMSA was performed as described in Figure 4. Open and closed arrowheads indicate Sp3-OND and Sp1-OND complex, respectively. Single and double asterisks indicate bands supershifted by the addition of Sp1 or Sp3 antibody, respectively.
(TIF)

Figure S5 The effect of mithramycin in MG63 cells. RNA was extracted from MG63 cells treated with mithramycin A at the indicated dose or DMSO for 48 h, and subjected to RT-PCR. The *β-actin* gene was used as a control.
(TIF)

Figure S6 Western blot analyses of AFAP1L1, Sp1 and Sp3 in sarcoma cell lines. Total cell lysate (A) or nuclear extract (B) was prepared from each cell line and used for Western blotting. β-tubulin and acetylated H3K9 were used as the internal control for total cell lysate and nuclear extract, respectively. Single and double asterisks indicate the long and short forms of the Sp3 protein, respectively.
(TIF)

Figure S7 The effect of Ets transcription factors on the expression of *AFAP1L1*. (A) The effect of Ets transcription factors on luciferase activity. Luciferase assays were performed in U2OS cells 48 h after the co-transfection of various expression vectors containing an Ets transcription factor with PGV-(−224). (B) The effect of ELK1 on the expression of Sp3. 293T cells were transfected with indicated plasmids and proteins were analyzed at 24 h by Western blotting. β-tubulin was used as an internal control. Single and double asterisks indicate the long and short forms of Sp3, respectively. DN-Ets represents dominant negative Ets. (C) Expression of ELK family gene in sarcoma cells. RNA was extracted from cells and RT-PCR was performed.
(TIF)

Figure S8 Down-regulation of *AFAP1L1* expression by siRNA targeting the *Sp3* gene in SYO-1 and MG63 cells. (A) and (D) The specificity of siRNA. SYO-1 (A) and MG63 (D) cells were treated with siRNA targeting *Sp1*, *Sp3*, or *Sp4* for 48 h, and the expression of these genes as well as the *AFAP1L1* gene was analyzed by PCR. Two different siRNAs targeting the *Sp1* and *Sp3* genes were designed and used. *β-actin* was used as a control. (B) and (E) Down-regulation of *AFAP1L1* expression by siRNA targeting the *Sp3* gene at the mRNA level. SYO-1 (B) and MG63 (E) cells were treated with siRNAs targeting each gene for 48 h and the expression of *AFAP1L1* was analyzed by qPCR and indicated as fold changes relative to that in untreated cells. (C) and (F) Down-regulation of AFAP1L1 expression by siRNA targeting the *Sp3* gene at the protein level. SYO-1 (C) and MG63 (F) cells were treated with siRNAs targeting each gene for 72 h and proteins were extracted and used for Western blotting. β-actin was used as a control.
(TIF)

Figure S9 Down-regulation of Sp3 expression causes down-regulation of AFAP1L1 expression in prostate cancer cells. (A) The specificity of siRNA. PC-3 cells were treated with siRNA targeting *Sp1*, *Sp3*, or *Sp4* for 48 h, and the expression of these genes as well as the *AFAP1L1* gene was analyzed by PCR. Two different siRNAs targeting the *Sp1* or *Sp3* gene were designed and used. *β-actin* was used as a control. (B) Down-regulation of AFAP1L1 expression by siRNA targeting the *Sp3* gene at the protein level. PC-3 cells were treated with siRNA targeting each gene for 72 h and proteins were extracted and used for Western blotting. β-tubulin was used as a control. Single and double asterisks indicate the long and short forms of Sp3, respectively.
(TIF)

Table S1 Sequences for primers and other oligonucleotides used in this study.
(XLS)

Acknowledgments

We thank Dr. Y. Jin and Mrs. Y. Kobayashi for technical support and Dr. M. Ikeya for editing the manuscript.

Author Contributions

Conceived and designed the experiments: YK HN EN OO JT. Performed the experiments: YK MF ST TK RT SN TA. Analyzed the data: YK JT. Contributed reagents/materials/analysis tools: TK YN JT. Wrote the paper: YK JT.

References

1. Furu M, Kajita Y, Nagayama S, Ishibe T, Shima Y, et al. (2011) Identification of AFAP1L1 as a prognostic marker for spindle cell sarcomas. Oncogene 30: 4015–4025.
2. Kawai A, Naito N, Yoshida A, Morimoto Y, Ouchida M, et al. (2004) Establishment and characterization of a biphasic synovial sarcoma cell line, SYO-1. Cancer Lett 204: 105–113.
3. Kato, Jr T, Gotoh Y, Hoffmann A., Ono Y (2008) Negative regulation of constitutive NF-κB and JNK signaling by PKN1-mediated phosphorylation of TRAF1: Genes to Cells; 13: 509–520.
4. Kohno Y, Okaкmoto T, Ishibe T, Nagayama S, Shima Y, et al. (2006) Expression of claudin7 is tightly associated with epithelial structures in synovial sarcomas and regulated by an Ets family transcription factor, ELF3. J Biol Chem 281: 38941–38950.
5. Sapetschnig A, Koch F, Rischitor G, Mennenga T, Suske G (2004) Complexity of translationally controlled transcription factor Sp3 isoform expression. J Biol Chem 279: 42095–42105.
6. Aoyama T, Okamoto T, Kohno Y, Fukiage K, Otsuka S, et al. (2008) Cell-specific epigenetic regulation of ChM-I gene expression: crosstalk between DNA methylation and histone acetylation. Biochem Biophys Res Commun 365: 124–130.
7. Sandelin A, Wasserman WW, Lenhard B (2004) ConSite: web-based prediction of regulatory elements using cross-species comparison. Nucleic Acids Res 32: W249–252.
8. Giatzakis C, Batarseh A, Dettin L, Papadopoulos V (2007) The role of Ets transcription factors in the basal transcription of the translocator protein (18 kDa). Biochemistry 46: 4763–4774.
9. Shirasaki F, Makhluf HA, LeRoy C, Watson DK, Trojanowska M (1999) Ets transcription factors cooperate with Sp1 to activate the human tenascin-C promoter. Oncogene 18: 7755–7764.
10. Blume SW, Snyder RC, Ray R, Thomas S, Koller CA, et al. (1991) Mithramycin inhibits SP1 binding and selectively inhibits transcriptional activity of the dihydrofolate reductase gene in vitro and in vivo. J Clin Invest 88: 1613–1621.
11. Ray R, Snyder RC, Thomas S, Koller CA, Miller DM (1989) Mithramycin blocks protein binding and function of the SV40 early promoter. J Clin Invest 83: 2003–2007.
12. Xu J, Bai XH, Lodyga M, Han B, Xiao H, et al. (2007) XB130, a novel adaptor protein for signal transduction. J Biol Chem 282: 16401–16412.
13. Flynn DC, Leu TH, Reynolds AB, Parsons JT (1993) Identification and sequence analysis of cDNAs encoding a 110-kilodalton actin filament-associated pp60src substrate. Mol Cell Biol 13: 7892–7900.
14. Lodyga M, De Falco V, Bai XH, Kapus A, Melillo RM, et al. (2009) XB130, a tissue-specific adaptor protein that couples the RET/PTC oncogenic kinase to PI 3-kinase pathway. Oncogene 28: 937–949.
15. Snyder BN, Cho Y, Qian Y, Coad JE, Flynn DC, et al. (2011) AFAP1L1 is a novel adaptor protein of the AFAP family that interacts with cortactin and localizes to invadosomes. Eur J Cell Biol 90: 376–389.
16. Suske G (1999) The Sp-family of transcription factors. Gene 238: 291–300.
17. Kadonaga JT, Carner KR, Masiarz FR, Tjian R (1987) Isolation of cDNA encoding transcription factor Sp1 and functional analysis of the DNA binding domain. Cell 51: 1079–1090.
18. Yu B, Datta PK and Bagchi S (2003) Stability of the Sp3-DNA is promoter-specific: Sp3 efficiently competes with Sp1 for binding to promoters containing multiple Sp-sites. Nucleic Acids Res 31: 5368–5376
19. Safe S, Abdelrahim M (2005) Sp transcription factor family and its role in cancer. Eur J Cancer 41: 2438–2448.
20. Wang L, Wei D, Huang S, Peng Z, Le X, et al. (2003) Transcription factor Sp1 expression is a significant predictor of survival in human gastric cancer. Clin Cancer Res 9: 6371–6380.
21. Chiefari E, Brunetti A, Arturi F, Bidart JM, Russo D, et al. (2002) Increased expression of AP2 and Sp1 transcription factors in human thyroid tumors: a role in NIS expression regulation? BMC Cancer 2: 35.
22. Hosoi Y, Watanabe T, Nakagawa K, Matsumoto Y, Enomoto A, et al. (2004) Up-regulation of DNA-dependent protein kinase activity and Sp1 in colorectal cancer. Int J Oncol 25: 461–468.
23. Abdelrahim M, Smith R 3rd, Burghardt R, Safe S (2004) Role of Sp proteins in regulation of vascular endothelial growth factor expression and proliferation of pancreatic cancer cells. Cancer Res 64: 6740–6749.
24. Wright C, Angus B, Napier J, Wetherall M, Udagawa Y, et al. (1987) Prognostic factors in breast cancer: immunohistochemical staining for SP1 and NCRC 11 related to survival, tumour epidermal growth factor receptor and oestrogen receptor status. J Pathol 153: 325–331.
25. Essafi-Benkhadir K, Grosso S, Puissant A, Robert G, Essafi M, et al. (2009) Dual role of Sp3 transcription factor as an inducer of apoptosis and a marker of tumour aggressiveness. PLoS One 4: e4478.
26. Barretina J, Taylor BS, Banerji S, Ramos AH, Lagos-Quintana M, et al. (2010) Subtype-specific genomic alterations define new targets for soft-tissue sarcoma therapy. Nat Genet 42: 715–721.
27. Detwiller KY, Fernando NT, Segal NH, Ryeom SW, D'Amore PA, et al. (2005) Analysis of hypoxia-related gene expression in sarcomas and effect of hypoxia on RNA interference of vascular endothelial cell growth factor A. Cancer Res 65: 5881–5889.

Molecular features of triple negative breast cancer cells by genome-wide gene expression profiling analysis

MASATO KOMATSU[1,2*], TETSURO YOSHIMARU[1*], TAISUKE MATSUO[1], KAZUMA KIYOTANI[1], YASUO MIYOSHI[3], TOSHIHITO TANAHASHI[4], KAZUHITO ROKUTAN[4], RUI YAMAGUCHI[5], AYUMU SAITO[6], SEIYA IMOTO[6], SATORU MIYANO[6], YUSUKE NAKAMURA[7], MITSUNORI SASA[8], MITSUO SHIMADA[2] and TOYOMASA KATAGIRI[1]

[1]Division of Genome Medicine, Institute for Genome Research, The University of Tokushima; [2]Department of Digestive and Transplantation Surgery, The University of Tokushima Graduate School; [3]Department of Surgery, Division of Breast and Endocrine Surgery, Hyogo College of Medicine, Hyogo 663-8501; [4]Department of Stress Science, Institute of Health Biosciences, The University of Tokushima Graduate School, Tokushima 770-8503; Laboratories of [5]Sequence Analysis, [6]DNA Information Analysis and [7]Molecular Medicine, Human Genome Center, Institute of Medical Science, The University of Tokyo, Tokyo 108-8639; [8]Tokushima Breast Care Clinic, Tokushima 770-0052, Japan

Received September 22, 2012; Accepted November 6, 2012

DOI: 10.3892/ijo.2012.1744

Abstract. Triple negative breast cancer (TNBC) has a poor outcome due to the lack of beneficial therapeutic targets. To clarify the molecular mechanisms involved in the carcinogenesis of TNBC and to identify target molecules for novel anticancer drugs, we analyzed the gene expression profiles of 30 TNBCs as well as 13 normal epithelial ductal cells that were purified by laser-microbeam microdissection. We identified 301 and 321 transcripts that were significantly upregulated and downregulated in TNBC, respectively. In particular, gene expression profile analyses of normal human vital organs allowed us to identify 104 cancer-specific genes, including those involved in breast carcinogenesis such as *NEK2, PBK* and *MELK*. Moreover, gene annotation enrichment analysis revealed prominent gene subsets involved in the cell cycle, especially mitosis. Therefore, we focused on cell cycle regulators, asp (abnormal spindle) homolog, microcephaly-associated (*Drosophila*) (*ASPM*) and centromere protein K (*CENPK*) as novel therapeutic targets for TNBC. Small-interfering RNA-mediated knockdown of their expression significantly attenuated TNBC cell viability due to G1 and G2/M cell cycle arrest. Our data will provide a better understanding of the carcinogenesis of TNBC and could contribute to the development of molecular targets as a treatment for TNBC patients.

Correspondence to: Dr Toyomasa Katagiri, Division of Genome Medicine, Institute of Genome Research, The University of Tokushima, 3-18-15 Kuramoto-cho, Tokushima 770-8503, Japan
E-mail: tkatagi@genome.tokushima-u.ac.jp

*Contributed equally

Key words: triple negative breast cancer, expression profiling, molecular targets

Introduction

Breast cancer is one of the most common solid malignant tumors among women worldwide. Breast cancer is a heterogeneous disease that is currently classified based on the expression of estrogen receptor (ER), progesterone receptor (PgR), and the human epidermal growth factor receptor 2 (HER2) (1,2). For patients with ER- or PgR-positive breast cancer, approximately five years of adjuvant endocrine therapy reduces the annual breast cancer death rate by approximately 30% (3). The addition of HER2-antagonist trastuzumab to adjuvant chemotherapy has improved the prognosis of HER2-positive breast cancer patients (4-6). In contrast, triple negative breast cancer (TNBC), defined as tumors that are negative for ER, PgR and HER2 overexpression, accounts for at least 15-20% of all breast cancers, and the prognosis for TNBC patients is poor because of its propensity for recurrence and metastasis and a lack of clinically-established targeted therapies (7,8). Therefore, only neoadjuvant chemotherapy with conventional cytotoxic agents yield an excellent outcome for TNBC patients who have a complete pathological response, but the outcome for the vast majority with residual disease after chemotherapy is relatively poor compared to non-TNBC patients (6,7). Thus, because the heterogeneity of breast cancer makes it difficult to treat many subtypes, including TNBC, the molecular mechanisms of the carcinogenesis of TNBC must be elucidated to develop novel molecular-targeted therapies that improve the clinical outcome of TNBC patients.

Current 'omics' technology including DNA microarray analysis can provide very helpful information that can be used to categorize the characteristics of various malignant tumors and identify genes that may be applicable for the develop-

ment of novel molecular targets for therapeutic modalities (9). To this end, we analyzed the gene expression profile of 30 TNBC cells and normal breast ductal cells that were purified by laser-microbeam microdissection and identified a number of cancer-specific genes that might contribute to the carcinogenesis of TNBC. TNBC gene expression profiling analysis can provide comprehensive information on the molecular mechanism underlying the carcinogenesis of TNBC and possibly lead to the development of novel effective therapies.

Materials and methods

Clinical samples and cell lines. A total of 48 TNBC (18 cases did not entry DNA microarray analysis) and 13 normal mammary tissues were obtained with informed consent from patients who were treated at Tokushima Breast Care Clinic, Tokushima, Japan. This study, as well as the use of all clinical materials described above, was approved by the Ethics Committee of The University of Tokushima. Clinical information was obtained from medical records and tumors were diagnosed as triple-negative by pathologists when immunohistochemical staining was ER-negative, PR-negative, and HER2 (0 or 1+). The clinicopathological features of each patient are summarized in Table I. Samples were immediately embedded in TissueTek OCT compound (Sakura, Tokyo, Japan), frozen, and stored at -80˚C. Human TNBC cell lines MDA-MB-231, BT-20, BT-549, HCC1143, and HCC1937 were purchased from the American Type Culture Collection (ATCC, Rockville, MD, USA). The human normal breast epithelial cell line, MCF10A, was purchased from Cambrex Bioscience, Inc. All cells were cultured under the conditions recommended by their respective depositors.

Laser-microbeam microdissection (LMM), RNA extraction, RNA amplification, and hybridization. Frozen specimens were serially sectioned in 8-μm slices with a cryostat (Leica, Herborn, Germany) and stained with hematoxylin and eosin to define the analyzed regions. We purified 48 TNBC and 13 normal ductal cells using the LMM system (Carl Zeiss, Jena, Germany) according to the manufacturer's instructions. Dissected cancer and normal ductal cells were dissolved in RLT lysis buffer (Qiagen, Valencia, CA, USA) containing 1% β-mercaptoethanol. The extracted total RNA was purified with an RNeasy Mini kit (Qiagen) according to the manufacturer's instructions. For RNA amplification and labeling, we used an Agilent Low-Input QuickAmp labeling kit according to the manufacturer's instructions. Briefly, 100 ng of total RNA from each sample was amplified using T7 RNA polymerase with simultaneous Cy3-labeled CTP incorporation. Then, 2 μg of Cy3-labeled cRNA was fragmented, hybridized onto the Agilent Whole Human Genome Microarray 4x44K slide (Agilent Technologies, Palo Alto, CA, USA) and then incubated with rotation at 65˚C for 18 h. Then slides were washed and scanned by the Agilent Microarray scanner system in an ozone protection fume hood.

Microarray analysis. The features of scanned image files containing the Cy3-fluorescence signals of the hybridized Agilent Microarrays were extracted using the Agilent Feature Extraction (version 9.5) (Agilent Technologies). The data were analyzed using GeneSpring (version 11.5). We normalized the microarray data across all chips and genes by quantile normalization, and baseline transformed the signal values to the median in all samples. Finally, we performed quality control and filtering steps based on flags and expression levels. To identify genes that were significantly alternated between TNBC and normal ductal cells the mean signal intensity values in each analysis were compared. In this experiment, we applied Mann-Whitney (unpaired) t-test and random permutation test 10,000 times for each comparison and adjusted for multiple comparisons using the Benjamini Hochberg false discovery rate (FDR). Gene expression levels were considered significantly different when the FDR (corrected P-value) $<5x10^{-4}$ (when comparing normal ductal cells and TNBC) and the fold change was ≥5.0. Data from this microarray analysis has been submitted to the NCBI Gene Expression Omnibus (GEO) archive as series GSE38959.

Functional gene annotation clustering. The Database for Annotation, Visualization and Integrated Discovery (DAVID 6.7) was approved to detect functional gene annotation clusters based on gene expression profiling by gene annotation enrichment analysis (http://david.abcc.ncifcrf.gov/) (10,11). The clusters from the gene annotation enrichment analysis were selected in this study based on a previous report (12).

Quantitative reverse transcription-PCR (qRT-PCR) analysis. Total RNA was extracted from each TNBC cell line and clinical sample using an RNeasy mini kit (Qiagen) according to the manufacturer's instructions. Purified RNA from each clinical sample and cell line, as well as poly-A RNA from normal human heart, lung, liver, and kidney (Takara, Otsu, Japan) was reverse transcribed for single-stranded cDNA using oligo(dT)$_{12-18}$ primers with Superscript II reverse transcriptase (Invitrogen, Life Technologies, Carlsbad, CA, USA). qRT-PCR analysis was performed using an ABI PRISM 7500 Real-Time PCR system (Applied Biosystems, Life Technologies, Carlsbad, CA, USA) and SYBR Premix Ex Taq (Takara) according to the manufacturer's instructions. The PCR primer sequences were as follows: 5'-GCAGGTCTCC TTTCCTTTGCT-3' and 5'-CTCGGCCTTCTTTGAGT GGT-3' for *ASPM*; 5'-CACTCACCGATTCAAATG CTC-3' and 5'-ACCACCGTTGTTCCCTTTCT-3' for *CENPK*; 5'-AAC TTAGAGGTGGGGAGCAG-3' and 5'-CACAACCATGCC TTACTTTATC-3' for *β2 microglobulin* (*β2-MG*) as a quantitative control.

Gene-silencing effect by RNA interference. Targeted sequences for *ASPM* and *CENPK* were determined using an siRNA Targeted Finder (Applied Biosystems, Life Technologies; http://www.ambion.com/techlib/misc/siRNA_finder.html). The siRNA targeting sequences were 5'-CATACAGAAGT GCGAGAAA-3' for *ASPM*, 5'-CTCAGTCAATGGC AGAAAA-3' for *CENPK* and 5'-GCAGCACGACTTCT TCAAG-3' for *EGFP* as a control siRNA. Human TNBC cell lines, HCC1937, MDA-MB-231 and BT-20, were plated at a density of $1x10^4$ cells per well in 12-wells for the MTT assay and $3x10^4$ cells per well in 6-well plates for flow cytometry and RT-PCR analyses. Cells were transfected with 16.6 nM

Table I. Clinicopathological features of 48 TNBC patients.

ID	Age	Histology	TNM	Stage	ER/PgR/HER2	Microarray	RT-PCR
1	44	Papillo-tubular	T0N3M1	IV	-/-/0	Done	Done
8	79	DCIS	T1N0M0	I	-/-/0	Not done	Done
10	57	Papillo-tubular	T1N0M0	I	-/-/1+	Not done	Done
19	63	Solid-tubular	T1N0M0	I	-/-/0	Not done	Done
27	60	Solid-tubular	T2N1M0	II	-/-/0	Done	Done
42	59	Solid-tubular	T2N0M0	II	-/-/0	Not done	Done
44	79	Papillo-tubular	Recurrence	-	-/-/1+	Not done	Done
53	55	Papillo-tubular	T1N0M0	I	-/-/0	Not done	Done
54	77	Solid-tubular	T1N1M0	II	-/-/0	Not done	Done
56	28	Scirrhous	T2N1M0	II	-/-/0	Done	Done
57	58	Solid-tubular	T1N1M0	II	-/-/0	Not done	Done
60	54	Solid-tubular	T2N1M0	II	-/-/0	Done	Done
64	60	Papillo-tubular	T2N0M0	II	-/-/0	Not done	Done
66	59	Special type	T2N1M0	II	-/-/0	Not done	Done
78	45	Solid-tubular	T2N1M0	II	-/-/0	Done	Done
89	44	Papillo-tubular	Recurrence	-	-/-/0	Not done	Done
95	60	Solid-tubular	T1N0M0	I	-/-/0	Not done	Done
101	60	Scirrhous	T2N1M0	II	-/-/0	Not done	Done
110	77	Scirrhous	T2N1M0	II	-/-/1+	Not done	Done
116	70	Solid-tubular	T2N1M0	II	-/-/0	Done	Done
155	36	Solid-tubular	T1N1M0	II	-/-/0	Done	Done
225	49	Papillo-tubular	T2N1M0	II	-/-/1+	Not done	Done
252	49	Solid-tubular	T2N1M0	II	-/-/1+	Done	Done
253	49	Scirrhous	T2N1M0	II	-/-/0	Done	Done
265	80	Scirrhous	T1N1M0	II	-/-/0-1+	Done	Done
313	53	Scirrhous	T3N2M0	III	-/-/0	Done	Done
337	42	Solid-tubular	T2N1M0	II	-/-/1+	Done	Done
359	55	Papillo-tubular	T2N0M0	II	-/-/0	Done	Done
362	37	Papillo-tubular	T2N1M0	II	-/-/0	Done	Done
363	69	Papillo-tubular	T2N0M0	II	-/-/0	Done	Done
366	61	Special type	T2N1M0	II	-/-/0-1+	Done	Done
384	32	Papillo-tubular	T3N0M0	II	-/-/0	Done	Done
392	46	Papillo-tubular	T1N1M0	II	-/-/0	Done	Done
414	60	Papillo-tubular	T2N1M0	II	-/-/1+	Not done	Done
415	54	Solid-tubular	T2N0M0	II	-/-/1+	Done	Done
420	41	Solid-tubular	T3N0M0	II	-/-/0	Done	Done
423	70	Solid-tubular	T2N0M0	II	-/-/0	Done	Done
438	63	Solid-tubular	T3N0M0	II	-/-/0	Done	Done
445	39	Solid-tubular	T2N1M0	II	-/-/0	Done	Done
453	50	Solid-tubular	T2N1M0	II	-/-/0	Done	Done
481	59	Solid-tubular	T3N1M0	III	-/-/0	Done	Done
528	55	Solid-tubular	T2N1M0	II	-/-/0	Done	Done
535	58	Solid-tubular	T2N1M0	II	-/-/0	Not done	Done
553	71	Solid-tubular	T0N1M0	II	-/-/1+	Not done	Done
558	56	Solid-tubular	T2N1M0	II	-/-/0	Done	Done
562	64	Scirrhous	T2N0M0	II	-/-/0	Done	Done
566	52	Solid-tubular	T3N1M0	III	-/-/0	Done	Done
651	45	Scirrhous	T2N1M0	II	-/-/0	Done	Done

DCIS, ductal carcinoma *in situ*; papillo-tubular, papillo-tubular adenocarcinoma; solid-tubular, solid-tubular adenocarcinoma; scirrhous, scirrhous carcinoma; special type ID 66, adenocarcinoma with squamous cell carcinoma; ID 366, osseous metaplasia; case 44, axillary lymph node metastasis was diagnosed 8 months after the first surgery followed by the dissection of metastatic lymph nodes; case 89, local recurrence in residual breast occurred after 2 years of the first surgery followed by a lumpectomy. All information was judged according to the General Rules for Clinical and Pathological Recording of Breast Cancer (The Japanese Breast Cancer Society). T, tumor stage; N, lymph node metastasis status; M, distant metastasis.

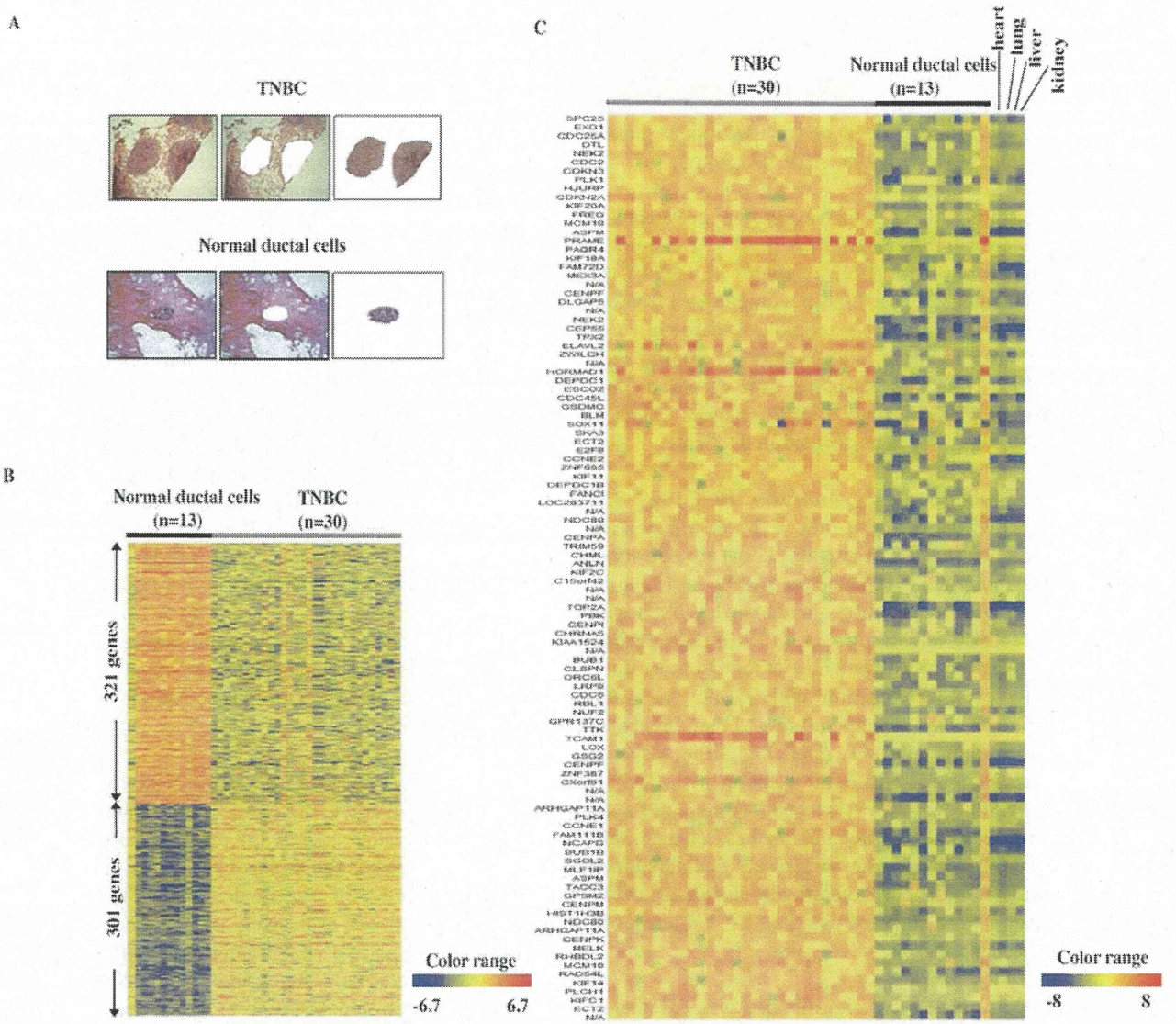

Figure 1. Purification of TNBC cells or ductal epithelial cells from normal ducts by means of microdissection and TNBC gene expression profiling. (A) Representative images of purified cancer cells and normal ductal epithelial cells from TNBC. Pre-microdissected (left lane), post-microdissected (middle lane) and microdissected cells (right lane) are shown after hematoxylin and eosin staining. (B) Heat-map image representing 622 genes that were significantly upregulated or downregulated >5-fold in TNBC. (C) Heat-map showing upregulated genes compared with normal ductal cells with no expression in normal organs including the heart, lung, liver and kidney.

of each siRNA using Lipofectamine RNAiMAX Reagent (Invitrogen). To evaluate the gene-silencing effects of the siRNAs by qRT-PCR, total RNA was extracted from the siRNA-transfected cells as described above after the indicated times. The following specific qRT-PCR primer sets were used: 5'-CGGAAAAGAAAGAGCGATGG-3' and 5'-ACCACCAAGTGAAGCCCTGT-3' for *ASPM* and 5'-GGGTGCCATCATTTTCTGGT-3' and 5'-CCACCGTTGTTCCCTTTCTAAG-3' for *CENPK*. To evaluate cell viability, the MTT assay was performed using the cell counting kit-8 reagent (Dojindo, Kumamoto, Japan) according to the manufacturer's instructions. Absorbance at 450 nm was measured with a micro-plate reader infinite 200 (Tecan, Männedorf, Switzerland). These experiments were performed in triplicate.

Colony formation assay. Vector-based shRNAs and the psiU6BX3 expression system were constructed as previously described (13). The shRNA target sequences were the same as those of the siRNA oligonucleotides. The DNA sequences of all constructs were confirmed by DNA sequencing. BT-20 and MDA-MB-231 cells were plated in 10-cm dishes ($1x10^6$ cells/dish) and transfected with 6 μg of psiU6BX3.0-*ASPM* or psiU6BX3.0-*CENPK* and psiU6BX3.0-*EGFP* as a control using Fugene-6 (Roche, Basel, Switzerland) according to the manufacturer's instructions. Forty-eight hours after transfection, cells were re-seeded for a colony formation assay ($5.0x10^5$ cells/10-cm dish) and RT-PCR ($5.0x10^5$ cells/10-cm dish). We selected psiU6BX3.0-transfected cells using selection medium containing 0.6 mg/ml of neomycin for BT-20 cells and 1.4 mg/ml for MDA-MB-231 cells. Total

RNA was extracted from the cells after a 7-day incubation with neomycin, and then the knockdown effects of the siRNAs were examined by qRT-PCR. The specific primer sets for quantitative RT-PCR were the same as those for the siRNA oligonucleotides. Nineteen days after transfection, the cells were fixed with 4% paraformaldehyde for 10 min and stained with Giemsa solution (Merck, Darmstadt, Germany).

Cell cycle analysis. For flow cytometric analysis, adherent and detached cells were harvested and fixed with 70% ethanol at room temperature for 30 min. After washing with PBS (-), the cells were incubated at 37°C for 30 min with 1 mg/ml RNase I in PBS (-) and stained with 20 μg propidium iodide at room temperature for 30 min in the dark. A total of 10,000 cells were analyzed for DNA content using flow cytometry and CellQuest software (FACSCalibur; BD Biosciences, Franklin Lakes, NJ, USA). Assays were performed in duplicate.

Immunocytochemical staining analysis. HCC1937 and MDA-MB-231 cells were plated onto a 2-well glass slide (Thermo Fisher Scientific, Rochester, NY, USA) at a density of $1.0x10^4$/well and incubated for 24 h before siRNA transfection. Forty-eight hours post-transfection, the cells were fixed with 4% paraformaldehyde for 30 min at 4°C and then permeablized with 0.1% Triton X-100 for 2 min at room temperature. Subsequently, the cells were covered with 3% bovine serum albumin for 60 min at room temperature and then incubated with an anti-α/β tubulin antibody (Cell Signaling, Beverly, MA, USA) diluted 1:50 for 1 h. After washing with PBS (-), the cells were stained with an Alexa 488-conjugated anti-rabbit secondary antibody (Molecular Probes, Eugene, OR, USA) diluted 1:1,000 for 1 h. The nuclei were counterstained with 4',6'-diamidine-2'-phenylindole dihydrochloride (DAPI). Fluorescent images were obtained using an IX71 microscope (Olympus, Tokyo, Japan).

Statistical analysis. Statistical significance was calculated by Mann-Whitney t-test using Stat View 5.0 J software (SAS Institute, Inc., Cary, NC, USA) to compare the gene expression levels between TNBC cells and normal ductal cells, and by Student's two-sided t-test using Microsoft® Excel 2008 to assess cell proliferation, gene expression, and alteration of cell cycle. A difference of $P<0.05$ was considered statistically significant.

Results

Identification of genes upregulated or downregulated in TNBCs. To obtain precise expression profiles of TNBC cells, we used LMM to avoid contamination of non-cancer cells, such as adipocytes, fibroblasts, and inflammatory cells from the tissue sections (Fig. 1A, upper panels). Because breast cancer originates from normal breast ductal cells, we used similarly purified populations of normal duct cells as controls (Fig. 1A, lower panels). The precise gene-expression profiles of TNBC by DNA microarray identified 301 genes that were upregulated >5-fold in TNBC compared to 13 normal ductal cells, and 321 genes that were downregulated to <1/5 of the normal ductal cells (Fig. 1B). Table II lists the 301 upregulated genes in TNBC, including ubiquitin-conjugating enzyme E2C (*UBE2C*) (14), S100 calcium binding protein P (*S100P*) (15), ubiquitin carboxyl-terminal esterase L1 (ubiquitin thiolesterase) (*UCHL1*) (16), pituitary tumor-transforming 1 (*PTTG1*) (17), ubiquitin-conjugating enzyme E2T (*UBE2T*) (13), ubiquitin-like with PHD and ring finger domains 1 (*UHRF1*) (18), SIX homeobox 1 (*SIX1*) (19), and protein regulator of cytokinesis 1 (*PRC1*) (20), which were previously reported to be overexpressed in breast cancer and involved in mammary carcinogenesis. In particular, topoisomerase (DNA) IIα (*TOP2A*) (21,22), HORMA domain containing 1 (*HORMAD1*) (23), ATPase family, Fatty acid binding protein 5 (psoriasis-associated) (*FABP5*) (24), and AAA domain containing 2 (*ATAD2*) (25) were previously reported to be potentially involved in the carcinogenesis of TNBC, and to serve as prognostic markers or therapeutic targets for TNBC.

On the other hand, Table III lists the 321 genes that were downregulated to <1/5 of normal ductal cells. Among these significantly downregulated genes, prolactin-induced protein (*PIP*) and dynein, axonemal, light intermediate chain 1 (*DNALI1*) were previously shown to be downregulated in TNBC (26). In particular, suppression of WNT inhibitory factor 1 (*WIF1*) (27) and signal peptide, CUB domain, EGF-like (*SCUBE2*) (28), both of which function as tumor suppressors, were among the genes that were downregulated as malignancy progressed. These data suggest that silencing or depletion of these genes might lead to the carcinogenesis of TNBC.

Identification of cancer-specific genes. Next, to develop novel therapeutic targets for TNBC with a minimum risk of adverse events, we performed a DNA microarray analysis of normal human vital organs consisting of the heart, lung, liver and kidney as well as TNBC cases and attempted to identify genes whose expression was exclusively upregulated in TNBC, but not expressed in normal vital organs. We identified 104 genes, which were specifically upregulated in TNBC, including cancer-specific molecules such as NIMA-related kinase 2 (*NEK2*) (29,30), PDZ binding kinase (*PBK*) (31), denticleless homolog (*Drosohila*) (*DTL*) (32), maternal leucine zipper kinase (*MELK*) (33), and kinesin family member C (*KIF2C*) (34), which have previously been shown to be involved in breast carcinogenesis (Fig. 1C and Table IV).

Functional gene annotation clustering analysis. To elucidate the biological processes and pathways characterized in TNBC, we performed a functional analysis of these upregulated or downregulated genes in 30 TNBC cases using the gene annotation clustering of the DAVID algorithm. We identified the most prominent cluster (cluster 1; gene enrichment score, 29.90) composed of various functional annotation terms consisting of 87 upregulated genes in TNBC (Table V). Cluster 1 consisted almost entirely of cell cycle-associated genes as represented by nuclear division (fold enrichment, 15.04), mitosis (fold enrichment, 15.04), M phase of the mitotic cell cycle (fold enrichment, 14.78), organelle fission (fold enrichment, 14.45), and M phase (fold enrichment, 12.90) (Fig. 2). These findings suggest that most of the upregulated genes in TNBC might be functionally responsible for cell cycle progression.

On the other hand, we also identified the most prominent cluster functionally deactivated in TNBC based on down-

Table II. Genes significantly upregulated in TNBC compared with normal ductal cells.

Probe ID	Accession no.	Symbol	Gene name	Fold change (log)	P-value
A_24_P334130	NM_054034	*FN1*	Fibronectin 1	5.33	1.26E-04
A_24_P940678	N/A	N/A		5.07	1.26E-04
A_23_P367618	NM_003412	*ZIC1*	Zic family member 1 (odd-paired homolog, *Drosophila*)	5.01	1.26E-04
A_23_P118834	NM_001067	*TOP2A*	Topoisomerase (DNA) IIα 170 kDa	4.76	1.26E-04
A_32_P119154	BE138567	N/A		4.75	1.26E-04
A_23_P35219	NM_002497	*NEK2*	NIMA (never in mitosis gene a)-related kinase 2	4.67	1.26E-04
A_23_P166360	NM_206956	*PRAME*	Preferentially expressed antigen in melanoma	4.64	1.26E-04
A_24_P332314	NM_198947	*FAM111B*	Family with sequence similarity 111, member B	4.63	1.26E-04
A_24_P413884	NM_001809	*CENPA*	Centromere protein A	4.59	1.26E-04
A_23_P68610	NM_012112	*TPX2*	TPX2, microtubule-associated, homolog (*Xenopus laevis*)	4.58	1.26E-04
A_23_P58266	NM_005980	*S100P*	S100 calcium binding protein P	4.57	1.26E-04
A_24_P297539	NM_181803	*UBE2C*	Ubiquitin-conjugating enzyme E2C	4.49	1.26E-04
A_23_P401	NM_016343	*CENPF*	Centromere protein F, 350/400 ka (mitosin)	4.44	1.26E-04
A_23_P57379	NM_003504	*CDC45L*	CDC45 cell division cycle 45-like (*S. cerevisiae*)	4.44	1.26E-04
A_23_P118815	NM_001012271	*BIRC5*	Baculoviral IAP repeat-containing 5	4.43	1.26E-04
A_23_P210853	NM_021067	*GINS1*	GINS complex subunit 1 (Psf1 homolog)	4.41	1.26E-04
A_23_P258493	NM_005573	*LMNB1*	Lamin B1	4.31	1.26E-04
A_24_P119745	NM_212482	*FN1*	Fibronectin 1	4.31	1.26E-04
A_24_P680947	BC044933	*KIF18B*	Kinesin family member 18B	4.3	1.26E-04
A_32_P92642	N/A	N/A		4.3	1.26E-04
A_23_P356684	NM_018685	*ANLN*	Anillin, actin binding protein	4.29	1.26E-04
A_24_P314571	BU616832	N/A		4.24	1.26E-04
A_23_P98580	NM_004265	*FADS2*	Fatty acid desaturase 2	4.2	1.26E-04
A_23_P52017	NM_018136	*ASPM*	asp (abnormal spindle) homolog, microcephaly associated (*Drosophila*)	4.17	1.26E-04
A_24_P20607	NM_005409	*CXCL11*	Chemokine (C-X-C motif) ligand 11	4.16	2.33E-04
A_32_P199884	NM_032132	*HORMAD1*	HORMA domain containing 1	4.13	2.33E-04
A_23_P70007	NM_012484	*HMMR*	Hyaluronan-mediated motility receptor (RHAMM)	4.11	1.26E-04
A_23_P22378	NM_003108	*SOX11*	SRY (sex determining region Y)-box 11	4.1	1.26E-04
A_23_P259586	NM_003318	*TTK*	TTK protein kinase	4.09	1.26E-04
A_23_P200310	NM_017779	*DEPDC1*	DEP domain containing 1	4.08	1.26E-04
A_24_P378331	NM_170589	*CASC5*	Cancer susceptibility candidate 5	4.06	1.26E-04
A_23_P111888	NM_138455	*CTHRC1*	Collagen triple helix repeat containing 1	4.05	1.26E-04
A_23_P48835	NM_138555	*KIF23*	Kinesin family member 23	4.05	1.26E-04
A_23_P115872	NM_018131	*CEP55*	Centrosomal protein 55 kDa	4.03	1.26E-04
A_23_P132956	NM_004181	*UCHL1*	Ubiquitin carboxyl-terminal esterase L1 (ubiquitin thiolesterase)	4.03	1.26E-04
A_24_P911179	NM_018136	*ASPM*	asp (abnormal spindle) homolog, microcephaly associated (*Drosophila*)	4.02	1.26E-04
A_23_P408955	NM_004091	*E2F2*	E2F transcription factor 2	4.02	1.26E-04
A_23_P7636	NM_004219	*PTTG1*	Pituitary tumor-transforming 1	4	1.26E-04
A_23_P204941	NM_004004	*GJB2*	Gap junction protein, β2, 26 kDa	4	1.26E-04
A_23_P18452	NM_002416	*CXCL9*	Chemokine (C-X-C motif) ligand 9	3.94	2.33E-04
A_24_P96780	NM_016343	*CENPF*	Centromere protein F, 350/400 ka (mitosin)	3.92	1.26E-04
A_23_P69537	NM_006681	*NMU*	Neuromedin U	3.9	1.26E-04

Table II. Continued.

Probe ID	Accession no.	Symbol	Gene name	Fold change (log)	P-value
A_24_P14156	NM_006101	*NDC80*	*NDC80* homolog, kinetochore complex component (*S. cerevisiae*)	3.86	1.26E-04
A_23_P254733	NM_024629	*MLF1IP*	MLF1 interacting protein	3.85	1.26E-04
A_23_P74115	NM_003579	*RAD54L*	RAD54-like (*S. cerevisiae*)	3.84	1.26E-04
A_23_P50108	NM_006101	*NDC80*	NDC80 homolog, kinetochore complex component (*S. cerevisiae*)	3.84	1.26E-04
A_24_P150160	NM_004265	*FADS2*	Fatty acid desaturase 2	3.83	1.26E-04
A_23_P155815	NM_022346	*NCAPG*	Non-SMC condensin I complex, subunit G	3.82	1.26E-04
A_23_P125278	NM_005409	*CXCL11*	Chemokine (C-X-C motif) ligand 11	3.81	1.26E-04
A_23_P51085	NM_020675	*SPC25*	SPC25, NDC80 kinetochore complex component, homolog (*S. cerevisiae*)	3.81	1.26E-04
A_23_P133123	NM_032117	*MND1*	Meiotic nuclear divisions 1 homolog (*S. cerevisiae*)	3.8	1.26E-04
A_32_P62997	NM_018492	*PBK*	PDZ binding kinase	3.8	1.26E-04
A_23_P256956	NM_005733	*KIF20A*	Kinesin family member 20A	3.79	1.26E-04
A_24_P933613	N/A	N/A		3.78	1.26E-04
A_23_P212844	NM_006342	*TACC3*	Transforming, acidic coiled-coil containing protein 3	3.78	1.26E-04
A_24_P254705	NM_020394	*ZNF695*	Zinc finger protein 695	3.76	1.26E-04
A_23_P115482	NM_014176	*UBE2T*	Ubiquitin-conjugating enzyme E2T (putative)	3.75	1.26E-04
A_32_P201723	N/A	N/A		3.73	1.26E-04
A_23_P256425	NM_014479	*ADAMDEC1*	ADAM-like, decysin 1	3.73	1.26E-04
A_23_P432352	NM_001017978	*CXorf61*	Chromosome X open reading frame 61	3.73	1.26E-04
A_23_P208880	NM_013282	*UHRF1*	Ubiquitin-like with PHD and ring finger domains 1	3.72	1.26E-04
A_23_P323751	NM_030919	*FAM83D*	Family with sequence similarity 83, member D	3.71	1.26E-04
A_23_P48669	NM_005192	*CDKN3*	Cyclin-dependent kinase inhibitor 3	3.71	1.26E-04
A_24_P234196	NM_001034	*RRM2*	Ribonucleotide reductase M2	3.69	1.26E-04
A_23_P253791	NM_004345	*CAMP*	Cathelicidin antimicrobial peptide	3.69	1.26E-04
A_23_P76914	NM_005982	*SIX1*	SIX homeobox 1	3.67	4.43E-04
A_23_P94571	NM_004432	*ELAVL2*	ELAV (embryonic lethal, abnormal vision, *Drosophila*)-like 2 (Hu antigen B)	3.67	1.26E-04
A_23_P200222	NM_033300	*LRP8*	Low density lipoprotein receptor-related protein 8, apolipoprotein E receptor	3.67	1.26E-04
A_24_P416079	NM_016359	*NUSAP1*	Nucleolar and spindle associated protein 1	3.66	1.26E-04
A_23_P104651	NM_080668	*CDCA5*	Cell division cycle associated 5	3.65	1.26E-04
A_23_P150667	NM_031217	*KIF18A*	Kinesin family member 18A	3.64	1.26E-04
A_24_P859859	N/A	N/A		3.63	4.43E-04
A_23_P312150	NM_001956	*EDN2*	Endothelin 2	3.61	1.26E-04
A_23_P375	NM_018101	*CDCA8*	Cell division cycle associated 8	3.59	1.26E-04
A_32_P68525	BC035392	N/A		3.58	1.26E-04
A_23_P43490	NM_058197	*CDKN2A*	Cyclin-dependent kinase inhibitor 2A (melanoma, p16, inhibits CDK4)	3.56	1.26E-04
A_23_P1691	NM_002421	*MMP1*	Matrix metallopeptidase 1 (interstitial collagenase)	3.55	1.26E-04
A_23_P117852	NM_014736	*KIAA0101*	KIAA0101	3.54	1.26E-04
A_24_P319613	NM_002497	*NEK2*	NIMA (never in mitosis gene a)-related kinase 2	3.53	1.26E-04
A_23_P10385	NM_016448	*DTL*	Denticleless homolog (*Drosophila*)	3.53	1.26E-04

Table II. Continued.

Probe ID	Accession no.	Symbol	Gene name	Fold change (log)	P-value
A_32_P1173	NM_138441	*C6orf150*	Chromosome 6 open reading frame 150	3.51	1.26E-04
A_23_P94422	NM_014791	*MELK*	Maternal embryonic leucine zipper kinase	3.5	1.26E-04
A_23_P340909	BC013418	*SKA3*	Spindle and kinetochore associated complex subunit 3	3.48	1.26E-04
A_23_P385861	NM_152562	*CDCA2*	Cell division cycle associated 2	3.47	1.26E-04
A_23_P124417	NM_004336	*BUB1*	Budding uninhibited by benzimidazoles 1 homolog (yeast)	3.47	1.26E-04
A_24_P257099	NM_018410	*HJURP*	Holliday junction recognition protein	3.43	1.26E-04
A_24_P270460	NM_005532	*IFI27*	Interferon, α-inducible protein 27	3.41	2.33E-04
A_23_P206059	NM_003981	*PRC1*	Protein regulator of cytokinesis 1	3.39	1.26E-04
A_23_P74349	NM_145697	*NUF2*	NUF2, NDC80 kinetochore complex component, homolog (*S. cerevisiae*)	3.36	1.26E-04
A_24_P302584	NM_003108	*SOX11*	SRY (sex determining region Y)-box 11	3.36	4.43E-04
A_24_P68088	NR_002947	*TCAM1*	Testicular cell adhesion molecule 1 homolog (mouse)	3.35	2.33E-04
A_24_P605612	NM_003247	*THBS2*	Thrombospondin 2	3.34	1.26E-04
A_24_P366033	NM_018098	*ECT2*	Epithelial cell transforming sequence 2 oncogene	3.34	1.26E-04
A_23_P93258	NM_003537	*HIST1H3B*	Histone cluster 1, H3b	3.33	1.26E-04
A_23_P211762	N/A	*COL8A1*	Collagen, type VIII, α1	3.29	4.43E-04
A_23_P77493	NM_006086	*TUBB3*	Tubulin, β3	3.29	1.26E-04
A_23_P204947	NM_004004	*GJB2*	Gap junction protein, β2, 26 kDa	3.29	1.26E-04
A_23_P149668	NM_014875	*KIF14*	Kinesin family member 14	3.29	1.26E-04
A_23_P34325	NM_033300	*LRP8*	Low density lipoprotein receptor-related protein 8, apolipoprotein E receptor	3.28	1.26E-04
A_32_P56154	N/A	N/A		3.28	1.26E-04
A_32_P10403	BU618641	*SERPINE1*	Serpin peptidase inhibitor, clade E (nexin, plasminogen activator inhibitor type 1), member 1	3.27	1.26E-04
A_23_P138507	NM_001786	*CDC2*	Cell division cycle 2, G1→S and G2→M	3.24	1.26E-04
A_23_P48513	NM_005532	*IFI27*	Interferon, α-inducible protein 27	3.23	1.26E-04
A_23_P49972	NM_001254	*CDC6*	Cell division cycle 6 homolog (*S. cerevisiae*)	3.22	1.26E-04
A_24_P306896	XR_040656	*LOC283711*	Hypothetical protein LOC283711	3.22	1.26E-04
A_23_P44684	NM_018098	*ECT2*	Epithelial cell transforming sequence 2 oncogene	3.21	1.26E-04
A_24_P161773	N/A	N/A		3.2	1.26E-04
A_23_P100344	NM_014321	*ORC6L*	Origin recognition complex, subunit 6 like (yeast)	3.2	1.26E-04
A_32_P162183	NM_000063	*C2*	Complement component 2	3.18	1.26E-04
A_23_P163481	NM_001211	*BUB1B*	Budding uninhibited by benzimidazoles 1 homolog β (yeast)	3.17	1.26E-04
A_32_P113784	N/A	N/A		3.16	1.26E-04
A_32_P87849	N/A	N/A		3.16	1.26E-04
A_24_P397107	NM_001789	*CDC25A*	Cell division cycle 25 homolog A (S. pombe)	3.15	1.26E-04
A_23_P209200	NM_001238	*CCNE1*	Cyclin E1	3.15	1.26E-04
A_32_P16625	N/A	N/A		3.15	1.26E-04
A_23_P58321	NM_001237	*CCNA2*	Cyclin A2	3.15	1.26E-04
A_24_P37903	N/A	*LOX*	Lysyl oxidase	3.12	1.26E-04

Table II. Continued.

Probe ID	Accession no.	Symbol	Gene name	Fold change (log)	P-value
A_32_P64919	NM_001042517	*DIAPH3*	Diaphanous homolog 3 (*Drosophila*)	3.12	1.26E-04
A_23_P379614	NM_007280	*OIP5*	Opa interacting protein 5	3.12	1.26E-04
A_23_P206441	NM_000135	*FANCA*	Fanconi anemia, complementation group A	3.09	1.26E-04
A_23_P16915	NM_012413	*QPCT*	Glutaminyl-peptide cyclotransferase	3.09	1.26E-04
A_23_P137173	NM_021992	*TMSB15A*	Thymosin β 15a	3.07	1.26E-04
A_24_P313504	NM_005030	*PLK1*	Polo-like kinase 1 (*Drosophila*)	3.07	1.26E-04
A_23_P251421	NM_031942	*CDCA7*	Cell division cycle associated 7	3.06	1.26E-04
A_23_P252292	NM_006733	*CENPI*	Centromere protein I	3.04	1.26E-04
A_23_P158725	NM_001042422	SLC16A3	Solute carrier family 16, member 3 (monocarboxylic acid transporter 4)	3.04	1.26E-04
A_23_P57417	NM_005940	*MMP11*	Matrix metallopeptidase11 (stromelysin 3)	3.03	1.26E-04
A_24_P291044	N/A	N/A		3.02	1.26E-04
A_23_P343927	NM_175065	*HIST2H2AB*	Histone cluster 2, H2ab	3.01	1.26E-04
A_23_P63789	NM_032997	*ZWINT*	ZW10 interactor	3.01	1.26E-04
A_23_P123596	NM_000170	*GLDC*	Glycine dehydrogenase (decarboxylating)	3	1.26E-04
A_23_P88731	NM_002875	*RAD51*	RAD51 homolog (RecA homolog, *E. coli*) (*S. cerevisiae*)	3	1.26E-04
A_23_P161474	NM_182751	*MCM10*	Minichromosome maintenance complex component 10	2.99	1.26E-04
A_24_P303354	NM_021064	*HIST1H2AG*	Histone cluster 1, H2ag	2.98	1.26E-04
A_23_P10518	NM_016521	*TFDP3*	Transcription factor Dp family, member 3	2.98	1.26E-04
A_24_P247660	NM_001002033	*HN1*	Hematological and neurological expressed 1	2.97	1.26E-04
A_23_P134910	NM_003878	*GGH*	γ-glutamyl hydrolase (conjugase, folylpolygammaglutamyl hydrolase)	2.97	1.26E-04
A_32_P7193	N/A	N/A		2.97	1.26E-04
A_23_P49878	NM_019013	*FAM64A*	Family with sequence similarity 64, member A	2.96	1.26E-04
A_24_P359231	BC014312	*HIST1H2BJ*	Histone cluster 1, H2bj	2.95	1.26E-04
A_32_P140262	N/A	N/A		2.95	1.26E-04
A_23_P55270	NM_002988	*CCL18*	Chemokine (C-C motif) ligand 18 (pulmonary and activation-regulated)	2.95	1.26E-04
A_24_P462899	NM_001012507	*C6orf173*	Chromosome 6 open reading frame 173	2.94	1.26E-04
A_23_P502520	NM_172374	*IL4I1*	Interleukin 4 induced 1	2.94	1.26E-04
A_23_P253762	N/A	N/A		2.94	1.26E-04
A_23_P214908	AY374131	N/A		2.94	1.26E-04
A_24_P225534	NM_017821	*RHBDL2*	Rhomboid, veinlet-like 2 (*Drosophila*)	2.94	1.26E-04
A_23_P203419	NM_013402	*FADS1*	Fatty acid desaturase 1	2.94	1.26E-04
A_23_P150935	NM_005480	*TROAP*	Trophinin associated protein (tastin)	2.94	1.26E-04
A_24_P412088	NM_182751	*MCM10*	Minichromosome maintenance complex component 10	2.94	1.26E-04
A_23_P71727	NM_001827	*CKS2*	CDC28 protein kinase regulatory subunit 2	2.93	1.26E-04
A_23_P217236	NM_005342	*HMGB3*	High-mobility group box 3	2.92	1.26E-04
A_32_P109296	NM_152259	*C15orf42*	Chromosome 15 open reading frame 42	2.91	1.26E-04
A_23_P89509	NM_006461	*SPAG5*	Sperm associated antigen 5	2.91	1.26E-04
A_24_P563068	N/A	N/A		2.91	1.26E-04
A_23_P416468	NM_025049	*PIF1*	PIF1 5'-to-3' DNA helicase homolog (*S. cerevisiae*)	2.91	1.26E-04
A_24_P38895	NM_002105	*H2AFX*	H2A histone family, member X	2.9	1.26E-04
A_23_P52278	NM_004523	*KIF11*	Kinesin family member 11	2.89	1.26E-04
A_24_P144543	N/A	N/A		2.89	1.26E-04

Table II. Continued.

Probe ID	Accession no.	Symbol	Gene name	Fold change (log)	P-value
A_24_P71468	NM_012413	*QPCT*	Glutaminyl-peptide cyclotransferase	2.88	2.33E-04
A_23_P116123	NM_001274	*CHEK1*	CHK1 checkpoint homolog (S. pombe)	2.88	1.26E-04
A_32_P106235	N/A	N/A		2.87	1.26E-04
A_24_P139152	AL359062	*COL8A1*	Collagen, type VIII, α1	2.87	4.43E-04
A_23_P36831	NM_003979	*GPRC5A*	G protein-coupled receptor, family C, group 5, member A	2.87	1.26E-04
A_23_P387471	NM_005931	*MICB*	MHC class I polypeptide-related sequence B	2.85	1.26E-04
A_23_P9574	NM_018098	*ECT2*	Epithelial cell transforming sequence 2 oncogene	2.84	1.26E-04
A_24_P535256	AK001903	*INHBA*	Inhibin, βA	2.84	1.26E-04
A_24_P76521	AK056691	*GSG2*	germ cell associated 2 (haspin)	2.83	1.26E-04
A_23_P103795	NM_138959	*VANGL1*	vang-like 1 (van gogh, *Drosophila*)	2.83	1.26E-04
A_32_P74409	NM_001145033	*LOC387763*	Hypothetical protein LOC387763	2.83	1.26E-04
A_23_P100632	NM_001002033	*HN1*	Hematological and neurological expressed 1	2.83	1.26E-04
A_23_P126212	NM_022111	*CLSPN*	Claspin homolog (*Xenopus laevis*)	2.83	1.26E-04
A_24_P659113	NM_152523	*CCNYL1*	Cyclin Y-like 1	2.83	1.26E-04
A_24_P367227	NM_001144755	*MYBL1*	v-myb myeloblastosis viral oncogene homolog (avian)-like 1	2.82	1.26E-04
A_23_P162719	NM_030932	*DIAPH3*	Diaphanous homolog 3 (*Drosophila*)	2.81	1.26E-04
A_32_P221799	NM_003514	*HIST1H2AM*	Histone cluster 1, H2am	2.81	1.26E-04
A_23_P60120	NM_031415	*GSDMC*	Gasdermin C	2.81	2.33E-04
A_24_P902509	NM_018193	*FANCI*	Fanconi anemia, complementation group I	2.8	1.26E-04
A_23_P50096	NM_001071	*TYMS*	Thymidylate synthetase	2.79	1.26E-04
A_32_P143245	NM_001012507	*C6orf173*	Chromosome 6 open reading frame 173	2.79	1.26E-04
A_23_P155969	NM_014264	*PLK4*	Polo-like kinase 4 (*Drosophila*)	2.79	1.26E-04
A_23_P62021	N/A	N/A		2.78	1.26E-04
A_32_P183218	NM_153695	*ZNF367*	Zinc finger protein 367	2.77	1.26E-04
A_23_P46118	NM_001821	*CHML*	Choroideremia-like (Rab escort protein 2)	2.76	2.33E-04
A_23_P327643	N/A	N/A		2.75	1.26E-04
A_23_P375104	NM_018193	*FANCI*	Fanconi anemia, complementation group I	2.75	1.26E-04
A_23_P1823	NM_000280	*PAX6*	Paired box 6	2.75	1.26E-04
A_23_P168014	NM_021066	*HIST1H2AJ*	Histone cluster 1, H2aj	2.74	1.26E-04
A_24_P413126	NM_020182	*PMEPA1*	Prostate transmembrane protein, androgen induced 1	2.74	1.26E-04
A_23_P80032	NM_005225	*E2F1*	E2F transcription factor 1	2.74	1.26E-04
A_23_P215976	NM_057749	*CCNE2*	Cyclin E2	2.72	2.33E-04
A_32_P231415	AF132203	*SCD*	Stearoyl-CoA desaturase (δ-9-desaturase)	2.72	1.26E-04
A_23_P370989	NM_005914	*MCM4*	Minichromosome maintenance complex component 4	2.72	1.26E-04
A_23_P216429	NM_017680	*ASPN*	Asporin	2.71	1.26E-04
A_24_P195621	NR_027288	*LOC341056*	SUMO-1 activating enzyme subunit 1 pseudogene	2.71	1.26E-04
A_32_P151800	NM_207418	*FAM72D*	Family with sequence similarity 72, member D	2.7	1.26E-04
A_23_P122197	NM_031966	*CCNB1*	Cyclin B1	2.7	1.26E-04
A_23_P34788	NM_006845	*KIF2C*	Kinesin family member 2C	2.7	1.26E-04
A_32_P206698	NM_001826	*CKS1B*	CDC28 protein kinase regulatory subunit 1B	2.7	1.26E-04
A_23_P99292	NM_006479	*RAD51AP1*	RAD51 associated protein 1	2.7	1.26E-04
A_23_P133956	NM_002263	*KIFC1*	Kinesin family member C1	2.69	1.26E-04
A_32_P143496	N/A	N/A		2.69	1.26E-04
A_32_P163858	NM_005063	*SCD*	Stearoyl-CoA desaturase (δ-9-desaturase)	2.69	1.26E-04

Table II. Continued.

Probe ID	Accession no.	Symbol	Gene name	Fold change (log)	P-value
A_32_P175557	R01145	N/A		2.69	1.26E-04
A_23_P63618	NM_005063	*SCD*	Stearoyl-CoA desaturase (δ-9-desaturase)	2.69	1.26E-04
A_23_P88630	NM_000057	*BLM*	Bloom syndrome, RecQ helicase-like	2.68	1.26E-04
A_24_P276102	NM_183404	*RBL1*	Retinoblastoma-like 1 (p107)	2.68	1.26E-04
A_23_P135385	N/A	N/A		2.68	1.26E-04
A_23_P57658	NM_020386	*HRASLS*	HRAS-like suppressor	2.67	1.26E-04
A_23_P23303	NM_003686	*EXO1*	Exonuclease 1	2.67	1.26E-04
A_23_P88691	NM_000745	*CHRNA5*	Cholinergic receptor, nicotinic, α5	2.67	1.26E-04
A_24_P923381	NR_002219	*EPR1*	Effector cell peptidase receptor 1 (non-protein coding)	2.66	1.26E-04
A_23_P24444	NM_001360	*DHCR7*	7-dehydrocholesterol reductase	2.65	1.26E-04
A_23_P43157	NM_001080416	*MYBL1*	v-myb myeloblastosis viral oncogene homolog (avian)-like 1	2.65	2.33E-04
A_23_P88740	NM_018455	*CENPN*	Centromere protein N	2.64	1.26E-04
A_23_P131866	NM_198433	*AURKA*	Aurora kinase A	2.64	1.26E-04
A_23_P259641	NM_004456	*EZH2*	Enhancer of zeste homolog 2 (*Drosophila*)	2.64	1.26E-04
A_32_P72341	NM_173084	*TRIM59*	Tripartite motif-containing 59	2.62	1.26E-04
A_24_P227091	NM_004523	*KIF11*	Kinesin family member 11	2.61	1.26E-04
A_23_P145238	NM_080593	*HIST1H2BK*	Histone cluster 1, H2bk	2.61	1.26E-04
A_23_P136805	NM_014783	*ARHGAP11A*	Rho GTPase activating protein 11A	2.6	1.26E-04
A_23_P167997	NM_003518	*HIST1H2BG*	Histone cluster 1, H2bg	2.6	1.26E-04
A_23_P63402	NM_013296	*GPSM2*	G-protein signaling modulator 2 (AGS3-like, *C. elegans*)	2.6	1.26E-04
A_24_P192994	NM_013402	*FADS1*	Fatty acid desaturase 1	2.59	1.26E-04
A_23_P25559	NM_005845	*ABCC4*	ATP-binding cassette, sub-family C (CFTR/MRP), member 4	2.59	3.41E-04
A_23_P309381	NM_001040874	*HIST2H2AA4*	Histone cluster 2, H2aa4	2.59	1.26E-04
A_23_P35871	NM_024680	*E2F8*	E2F transcription factor 8	2.58	1.26E-04
A_23_P207307	N/A	N/A		2.58	1.26E-04
A_24_P399888	NM_001002876	*CENPM*	Centromere protein M	2.58	1.26E-04
A_23_P360754	NM_005099	*ADAMTS4*	ADAM metallopeptidase with thrombospondin type 1 motif, 4	2.57	3.41E-04
A_23_P21706	NM_001905	*CTPS*	CTP synthase	2.57	1.26E-04
A_24_P174924	NM_003537	*HIST1H3B*	Histone cluster 1, H3b	2.57	1.26E-04
A_23_P155989	NM_022145	*CENPK*	Centromere protein K	2.57	1.26E-04
A_23_P103981	NM_001040874	*HIST2H2AA4*	Histone cluster 2, H2aa4	2.56	1.26E-04
A_23_P571	NM_006516	*SLC2A1*	Solute carrier family 2 (facilitated glucose transporter), member 1	2.56	1.26E-04
A_23_P420551	NM_007174	*CIT*	Citron (rho-interacting, serine/threonine kinase 21)	2.56	1.26E-04
A_23_P411335	NM_152524	*SGOL2*	Shugoshin-like 2 (S. pombe)	2.54	1.26E-04
A_32_P147090	NM_199357	*ARHGAP11A*	Rho GTPase activating protein 11A	2.54	1.26E-04
A_23_P70448	NM_005325	*HIST1H1A*	Hstone cluster 1, H1a	2.53	1.26E-04
A_23_P43484	NM_058197	*CDKN2A*	Cyclin-dependent kinase inhibitor 2A (melanoma, p16, inhibits CDK4)	2.52	1.26E-04
A_24_P85539	NM_212482	*FN1*	Fibronectin 1	2.52	1.26E-04
A_32_P28704	N/A	N/A		2.52	1.26E-04
A_23_P107421	NM_003258	*TK1*	Thymidine kinase 1, soluble	2.51	1.26E-04
A_23_P502425	NM_020409	*MRPL47*	Mitochondrial ribosomal protein L47	2.5	1.26E-04

Table II. Continued.

Probe ID	Accession no.	Symbol	Gene name	Fold change (log)	P-value
A_24_P351466	NM_020890	*KIAA1524*	KIAA1524	2.5	1.26E-04
A_23_P211910	NM_182943	*PLOD2*	Procollagen-lysine, 2-oxoglutarate 5-dioxygenase 2	2.5	1.26E-04
A_24_P9321	NM_003533	*HIST1H3I*	Histone cluster 1, H3i	2.49	1.26E-04
A_24_P334248	NM_014996	*PLCH1*	Phospholipase C, eta 1	2.48	1.26E-04
A_24_P819890	NM_001005210	*LRRC55*	Leucine rich repeat containing 55	2.48	4.43E-04
A_23_P146456	NM_001333	*CTSL2*	Cathepsin L2	2.48	2.33E-04
A_24_P242440	NM_003780	*B4GALT2*	UDP-Gal:βGlcNAc β 1,4-galactosyltransferase, polypeptide 2	2.47	1.26E-04
A_23_P88331	NM_014750	*DLGAP5*	Discs, large (*Drosophila*) homolog-associated protein 5	2.47	1.26E-04
A_23_P216068	NM_014109	*ATAD2*	ATPase family, AAA domain containing 2	2.46	1.26E-04
A_32_P31021	N/A	N/A		2.46	1.26E-04
A_23_P373119	NR_002165	*HMGB3L1*	High-mobility group box 3-like 1	2.46	1.26E-04
A_23_P361419	NM_018369	*DEPDC1B*	DEP domain containing 1B	2.45	1.26E-04
A_23_P10870	NM_014908	*DOLK*	Dolichol kinase	2.44	1.26E-04
A_23_P420692	NM_015053	*PPFIA4*	Protein tyrosine phosphatase, receptor type, f polypeptide (PTPRF), interacting protein (liprin), α4	2.43	1.26E-04
A_23_P146284	NM_003129	*SQLE*	Squalene epoxidase	2.43	1.26E-04
A_32_P159254	AK123584	N/A		2.43	2.33E-04
A_23_P25626	NM_024808	*C13orf34*	Chromosome 13 open reading frame 34	2.43	1.26E-04
A_23_P59005	NM_000593	*TAP1*	Transporter 1, ATP-binding cassette, sub-family B (MDR/TAP)	2.43	2.33E-04
A_24_P49747	XM_929965	*LOC646993*	Similar to high mobility group box 3	2.43	1.26E-04
A_23_P252740	NM_024094	*DSCC1*	Defective in sister chromatid cohesion 1 homolog (*S. cerevisiae*)	2.42	1.26E-04
A_23_P397341	NM_152341	*PAQR4*	Progestin and adipoQ receptor family member IV	2.42	1.26E-04
A_23_P59045	NM_021052	*HIST1H2AE*	Histone cluster 1, H2ae	2.42	1.26E-04
A_23_P140316	NM_001099652	*GPR137C*	G protein-coupled receptor 137C	2.42	1.26E-04
A_23_P207520	Z74615	*COL1A1*	Collagen, type I, α1	2.41	1.26E-04
A_24_P920968	NM_182625	*GEN1*	Gen homolog 1, endonuclease (*Drosophila*)	2.41	1.26E-04
A_23_P366216	NM_003524	*HIST1H2BH*	Histone cluster 1, H2bh	2.41	1.26E-04
A_23_P217049	NM_014286	*FREQ*	Frequenin homolog (*Drosophila*)	2.41	2.33E-04
A_32_P194264	NM_001008708	*CHAC2*	ChaC, cation transport regulator homolog 2 (*E. coli*)	2.4	2.33E-04
A_32_P35839	N/A	N/A		2.4	1.26E-04
A_23_P154894	NM_000100	*CSTB*	Cystatin B (stefin B)	2.4	1.26E-04
A_24_P340066	NM_001421	*ELF4*	E74-like factor 4 (ets domain transcription factor)	2.4	1.26E-04
A_24_P857404	NM_001093725	*MEX3A*	mex-3 homolog A (*C. elegans*)	2.4	1.26E-04
A_24_P133488	NM_017955	*CDCA4*	Cell division cycle associated 4	2.4	1.26E-04
A_23_P339240	NM_014996	*PLCH1*	Phospholipase C, eta 1	2.39	2.33E-04
A_23_P52410	NM_145307	*RTKN2*	Rhotekin 2	2.39	1.26E-04
A_23_P59877	NM_001444	*FABP5*	Fatty acid binding protein 5 (psoriasis-associated)	2.39	1.26E-04
A_23_P29594	NM_052969	*RPL39L*	Ribosomal protein L39-like	2.38	1.26E-04
A_23_P11984	NM_201649	*SLC6A9*	Solute carrier family 6 (neurotransmitter transporter, glycine), member 9	2.38	2.33E-04
A_23_P200866	NM_203401	*STMN1*	Stathmin 1	2.37	1.26E-04

Table II. Continued.

Probe ID	Accession no.	Symbol	Gene name	Fold change (log)	P-value
A_32_P182135	N/A	N/A		2.36	1.26E-04
A_24_P323598	NM_001017420	*ESCO2*	Establishment of cohesion 1 homolog 2 (*S. cerevisiae*)	2.36	1.26E-04
A_23_P39574	NM_001080539	*CCDC150*	Coiled-coil domain containing 150	2.36	1.26E-04
A_24_P275386	AK025766	*BRI3BP*	BRI3 binding protein	2.36	1.26E-04
A_23_P85460	NM_078626	*CDKN2C*	Cyclin-dependent kinase inhibitor 2C (p18, inhibits CDK4)	2.35	1.26E-04
A_23_P57306	NM_005441	*CHAF1B*	Chromatin assembly factor 1, subunit B (p60)	2.35	1.26E-04
A_23_P335329	NM_004485	*GNG4*	Guanine nucleotide binding protein (G protein), γ4	2.35	2.33E-04
A_23_P92441	NM_002358	*MAD2L1*	MAD2 mitotic arrest deficient-like 1 (yeast)	2.35	1.26E-04
A_24_P13390	NM_032814	*RNFT2*	Ring finger protein, transmembrane 2	2.35	1.26E-04
A_23_P362046	NM_138779	*C13orf27*	Chromosome 13 open reading frame 27	2.34	1.26E-04
A_23_P24716	NM_017870	*TMEM132A*	Transmembrane protein 132A	2.34	1.26E-04
A_23_P91900	NM_005496	*SMC4*	structural maintenance of chromosomes 4	2.33	1.26E-04
A_24_P105102	NM_182687	*PKMYT1*	Protein kinase, membrane associated tyrosine/ threonine 1	2.33	1.26E-04
A_24_P244420	NM_018367	ACER3	alkaline ceramidase 3	2.33	2.33E-04
A_23_P112673	NM_017975	ZWILCH	Zwilch, kinetochore associated, homolog (*Drosophila*)	2.33	1.26E-04
A_23_P87769	NM_017915	*C12orf48*	Chromosome 12 open reading frame 48	2.33	1.26E-04
A_24_P296254	NM_014783	*ARHGAP11A*	Rho GTPase activating protein 11A	2.32	1.26E-04
A_23_P166306	NM_000071	*CBS*	Cystathionine-β-synthase	2.32	1.26E-04

N/A, not annotated; P-value, Benjamini-Hochberg false discovery rate of random permutation test; log fold change, between groups. Gene symbol, accession number and gene name were exported from GeneSpring (from the NCBI databases).

regulated genes in TNBC (cluster 2; enrichment score, 6.43). As shown in Table V and Fig. 2, cluster 2 consisted of functions induced by extracellular matrix-cell adhesion-associated genes such as latent transforming growth factor β binding protein 2 (*LTBP2*), laminin α3 (*LAMA3*) and cell adhesion molecule with homology to L1CAM (close homolog of L1) (*CHL1*), which have been reported to be downregulated in various tumors (35-37). These results suggest that loss of cell-cell or matrix-cell interactions might be a key mechanism in TNBC progression.

Identification of ASPM and CENPK as novel molecular targets for TNBC therapy. Because the upregulated genes were mainly included in the cell cycle-associated gene cluster as described above, we directed our focus to two cancer-specific genes that function as cell cycle regulators, asp (abnormal spindle) homolog, microcephaly associated (*Drosophila*) (*ASPM*), which is fundamental for cytokinesis (38) and centromere protein K (*CENPK*), which is essential for proper kinetochore assembly during mitosis (39), as novel therapeutic targets for TNBC. qRT-PCR experiments confirmed that *ASPM* and *CENPK* genes were significantly upregulated in 48 clinical TNBC cases (Fig. 3A) and five cell lines derived from TNBC (Fig. 3B), but undetectably expressed in a mixture of 13 microdissected normal mammary ductal cells and the normal mammary epithelial cell line MCF10A as well as normal human vital organs.

To ascertain the possible roles of *ASPM* and *CENPK* in TNBC cell growth, we knocked down the expression of endogenous *ASPM* and *CENPK* in three TNBC cell lines, HCC1937, BT-20 and MDA-MB-231 cells, which highly express both of these genes (Fig. 3), using RNAi. qRT-PCR experiments showed that *ASPM* and *CENPK* were significantly knocked down in cells transfected with si*ASPM* and si*CENPK*, but not with si*EGFP* as a control (Fig. 4A). In concordance with their knockdown, the MTT assay clearly revealed growth suppression of breast cancer cells in a time-dependent manner by si*ASPM* and si*CENPK*, compared with a control si*EGFP*, which showed no knockdown (Fig. 4B). In addition, a colony formation assay also confirmed that introducing both shRNA-*ASPM* and -*CENPK* constructs remarkably suppressed the growth of BT-20 and MDA-MB-231 cells, respectively, compared with sh*EGFP*-transfected cells (Fig. 4C), suggesting that both genes are likely indispensable for breast cancer cell growth. Furthermore, we investigated the phenotypic alterations of TNBC cells transfected with *ASPM* and *CENPK* siRNAs

Table III. Significantly downregulated genes in TNBC compared with normal ductal cells.

Probe ID	Accession no.	Symbol	Gene name	Fold change (log)	P-value
A_23_P127781	NM_006552	*SCGB1D1*	Secretoglobin, family 1D, member 1	-6.77	1.26E-04
A_32_P234405	CK570316	N/A		-6.62	1.26E-04
A_23_P150555	NM_006551	*SCGB1D2*	Secretoglobin, family 1D, member 2	-6.51	1.26E-04
A_23_P12533	NM_052997	*ANKRD30A*	Ankyrin repeat domain 30A	-6.44	1.26E-04
A_23_P8702	NM_002652	*PIP*	Prolactin-induced protein	-6.34	1.26E-04
A_23_P501010	NM_000494	*COL17A1*	Collagen, type XVII, α1	-5.69	1.26E-04
A_24_P844984	NM_002644	*PIGR*	Polymeric immunoglobulin receptor	-5.55	1.26E-04
A_32_P216520	NM_007191	*WIF1*	WNT inhibitory factor 1	-5.53	1.26E-04
A_23_P71364	NM_015886	*PI15*	Peptidase inhibitor 15	-5.33	1.26E-04
A_24_P273756	NM_003722	*TP63*	Tumor protein p63	-5.11	1.26E-04
A_23_P132619	NM_000916	*OXTR*	Oxytocin receptor	-4.89	1.26E-04
A_32_P111873	BQ432543	N/A		-4.88	1.26E-04
A_32_P23272	N/A	N/A		-4.85	1.26E-04
A_24_P643776	N/A	N/A		-4.74	1.26E-04
A_23_P136777	NM_001647	*APOD*	Apolipoprotein D	-4.71	1.26E-04
A_23_P9711	NM_006040	*HS3ST4*	Heparan sulfate (glucosamine) 3-O-sulfotransferase 4	-4.58	1.26E-04
A_23_P305292	NR_027180	*LOC728264*	Hypothetical LOC728264	-4.57	1.26E-04
A_23_P159974	NM_033495	*KLHL13*	Kelch-like 13 (*Drosophila*)	-4.55	1.26E-04
A_23_P105144	NM_020974	*SCUBE2*	Signal peptide, CUB domain, EGF-like 2	-4.51	1.26E-04
A_32_P14253	N/A	N/A		-4.47	1.26E-04
A_23_P327380	NM_003722	*TP63*	Tumor protein p63	-4.45	1.26E-04
A_23_P337270	AK057247	N/A		-4.43	1.26E-04
A_23_P420442	NM_153618	*SEMA6D*	Sema domain, transmembrane domain (TM), and cytoplasmic domain, (semaphorin) 6D	-4.34	1.26E-04
A_23_P8812	N/A	N/A		-4.3	1.26E-04
A_23_P160377	NM_003462	*DNALI1*	Dynein, axonemal, light intermediate chain 1	-4.26	1.26E-04
A_24_P92680	AK093340	*LOC100132116*	Hypothetical LOC100132116	-4.23	1.26E-04
A_23_P216779	NM_001007097	*NTRK2*	Neurotrophic tyrosine kinase, receptor, type 2	-4.23	1.26E-04
A_23_P148249	NM_024817	*THSD4*	Thrombospondin, type I, domain containing 4	-4.18	1.26E-04
A_23_P206920	NM_001040114	*MYH11*	Myosin, heavy chain 11, smooth muscle	-4.13	1.26E-04
A_32_P154473	NM_004522	*KIF5C*	Kinesin family member 5C	-4.13	1.26E-04
A_23_P128362	NM_206819	*MYBPC1*	Myosin binding protein C, slow type	-4.11	3.41E-04
A_23_P83381	NM_001143962	*CAPN8*	Calpain 8	-4.08	1.26E-04
A_23_P397208	NM_000848	*GSTM2*	Glutathione S-transferase mu 2 (muscle)	-4.07	1.26E-04
A_23_P503072	NM_148672	*CCL28*	Chemokine (C-C motif) ligand 28	-4.03	1.26E-04
A_23_P143068	NM_024726	*IQCA1*	IQ motif containing with AAA domain 1	-4.01	1.26E-04
A_24_P829209	AK096334	LOC285944	Hypothetical protein LOC285944	-3.99	2.33E-04
A_23_P394246		GPR81	G protein-coupled receptor 81	-3.96	1.26E-04
A_24_P34186	NM_004010	*DMD*	Dystrophin	-3.96	1.26E-04
A_23_P303087	NM_002825	*PTN*	Pleiotrophin	-3.95	1.26E-04
A_24_P243749	NM_002612	*PDK4*	Pyruvate dehydrogenase kinase, isozyme 4	-3.94	1.26E-04